

Improved genome assembly and pan-genome provide key insights into eggplant domestication and breeding

Lorenzo Barchi¹ , Mark Timothy Rabanus-Wallace² , Jaime Prohens³ , Laura Toppino⁴ , Sudharsan Padmarasu² , Ezio Portis¹ , Giuseppe Leonardo Rotino⁴ , Nils Stein^{2,5} , Sergio Lanteri¹  and Giovanni Giuliano^{6,*} 

¹DISAFA – Plant genetics, University of Turin, Grugliasco (TO) 10095, Italy,

²Leibniz Institute of Plant Genetics and Crop Plant Research (IPK), Corrensstr. 3, Seeland 06466, Germany,

³COMAV, Universitat Politècnica de València, Camino de Vera 14, Valencia 46022, Spain,

⁴CREA Research Centre for Genomics and Bioinformatics, Via Pausanias 28, Montanaso Lombardo, LO 26836, Italy,

⁵Department of Crop Sciences, Center for Integrated Breeding Research (CiBreed), Georg-August-University, Von Siebold Str. 8, Göttingen 37075, Germany, and

⁶ENEA, Casaccia Res Ctr, Via Anguillarese 301, Rome 00123, Italy

Received 21 January 2021; revised 30 April 2021; accepted 4 May 2021.

*For correspondence (e-mail giovanni.giuliano@enea.it).

SUMMARY

Eggplant (*Solanum melongena* L.) is an important horticultural crop and one of the most widely grown vegetables from the Solanaceae family. It was domesticated from a wild, prickly progenitor carrying small, round, non-anthocyanic fruits. We obtained a novel, highly contiguous genome assembly of the eggplant '67/3' reference line, by Hi-C retrofitting of a previously released short read- and optical mapping-based assembly. The sizes of the 12 chromosomes and the fraction of anchored genes in the improved assembly were comparable to those of a chromosome-level assembly. We resequenced 23 accessions of *S. melongena* representative of the worldwide phenotypic, geographic, and genetic diversity of the species, and one each from the closely related species *Solanum insanum* and *Solanum incanum*. The eggplant pan-genome contained approximately 51.5 additional megabases and 816 additional genes compared with the reference genome, while the pan-plastome showed little genetic variation. We identified 53 selective sweeps related to fruit color, prickliness, and fruit shape in the nuclear genome, highlighting selection leading to the emergence of present-day *S. melongena* cultivars from its wild ancestors. Candidate genes underlying the selective sweeps included a *MYBL1* repressor and *CHALCONE ISOMERASE* (for fruit color), homologs of Arabidopsis *GLABRA1* and *GLABROUS INFLORESCENCE STEMS2* (for prickliness), and orthologs of tomato *FW2.2*, *OVATE*, *LOCULE NUMBER/WUSCHEL*, *SUPPRESSOR OF OVATE*, and *CELL SIZE REGULATOR* (for fruit size/shape), further suggesting that selection for the latter trait relied on a common set of orthologous genes in tomato and eggplant.

Keywords: *Solanum melongena*, genome assembly, whole-genome resequencing, pan-genome, pan-plastome, domestication, single nucleotide polymorphism, indel, eggplant wild relatives.

INTRODUCTION

With a worldwide production of more than 54 megatons, common eggplant (*Solanum melongena* L.) is an important horticultural crop and the third most cultivated Solanaceae species, after potato (*Solanum tuberosum* L.) and tomato (*Solanum lycopersicum* L.) (FAO). Within the genus *Solanum*, eggplant and its relatives are part of subgenus *Leptostemonum*, collectively known as the 'spiny solanum' group (Vorontsova *et al.*, 2013). Species from the eggplant clade, such as the direct wild ancestor *Solanum insanum*

L. and the sister species *Solanum incanum* L., are closely related to *S. melongena*. More distant species from the Anguivi grade include the two other cultivated eggplant species: the scarlet eggplant (*Solanum aethiopicum* L.) and the gboma eggplant (*Solanum macrocarpon* L.) (Acquadro *et al.*, 2017; Barchi *et al.*, 2019a; Vorontsova *et al.*, 2013).

Within the 'spiny solanum' group, non-anchored genome sequences are available for *S. melongena* (v1.0, Hirakawa *et al.*, 2014) and *S. aethiopicum* (Song *et al.*, 2019). A chromosome-anchored genome sequence (v3.0;

Barchi *et al.*, 2019b) and a chromosome-level (CL) assembly (Wei *et al.*, 2020a) of two different lines have been recently released for *S. melongena*, but improvement of the former sequence is still needed, due to the low proportion of anchored genes.

Common eggplant exhibits a wide range of phenotypic variation (Cericola *et al.*, 2014; Portis *et al.*, 2015) and metabolic diversity (Kaushik *et al.*, 2017). Similar to other species, individual cultivars/accessions of eggplant are expected to contain genes absent in the reference genome and *vice versa* (referred to as presence/absence variants [PAVs]). These variants are expected to affect phenotypic traits, and can be revealed by resequencing of different accessions. Within the Solanaceae, pan-genome resequencing projects have been undertaken in pepper (*Capsicum annuum* L.) (Ou *et al.*, 2018), tomato (Gao *et al.*, 2019) and *S. aethiopicum* (Song *et al.*, 2019).

Quantitative trait locus (QTL) mapping in eggplant has been undertaken using germplasm sets as well as progeny populations from both intra- and interspecific crosses (Barchi *et al.*, 2012; Barchi *et al.*, 2018; Doganlar *et al.*, 2002b; Frary *et al.*, 2003; Frary *et al.*, 2014; Mangino *et al.*, 2020; Mangino *et al.*, 2021; Miyatake *et al.*, 2012; Nunome *et al.*, 2001; Portis *et al.*, 2014; Salgon *et al.*, 2018; Toppino *et al.*, 2016; Toppino *et al.*, 2020; Wei *et al.*, 2020b). Several QTLs for eggplant fruit weight, shape, and color have been found at orthologous positions with respect to those from tomato, potato, or pepper, suggesting a common genetic basis for some fruit traits in Solanaceae (Chapman, 2019; Doğanlar *et al.*, 2014; Doganlar *et al.*, 2002a; Mangino *et al.*, 2021).

Sequencing of whole plastomes and selected plastid regions allows the construction of phylogenies at the species and, occasionally, at the subspecies level (Lakušić *et al.*, 2013; Magdy *et al.*, 2019; Parks *et al.*, 2009). Plastid DNA consists of a circular chromosome comprised of a pair of inverted repeats (IRs) separated by two single-copy regions. Currently, 145 Solanaceae plastid genomes are available in the National Center for Biotechnology Information (NCBI) database, including those of *S. melongena*, *S. incanum*, *S. aethiopicum*, and *S. macrocarpon*. The availability of a large number of chloroplast sequences may contribute to the development of reproducible molecular markers for DNA barcoding, population-based studies, phylogeography, and domestication genetics.

Here, we report an improved, highly contiguous *S. melongena* reference genome (v4.0), obtained by scaffolding of v3.0 by the help of 3D chromosome conformation capture (Hi-C) information. In total, 23 *S. melongena* accessions, representative of the genetic and phenotypic diversity of the species, plus one accession each from the closest wild relatives *S. insanum* and *S. incanum* (non-*melongena* species [NMSs]) were resequenced to deduce a first eggplant pan-genome and pan-plastome. We used

this information to estimate the genetic variability of nuclear and plastid sequences, identify additional genes absent in the reference genome (i.e., PAVs), compare the congruence of nuclear- and plastid-based phylogenies, and identify selective sweeps (SSs) associated with the selection of key agronomic traits in *S. melongena*.

RESULTS

Assembly of the Smel v4.0 genome

A total of 118191133 paired-end reads were generated, and after adapter trimming and quality control, 26 759 980 valid Hi-C links were identified (Figure S1(a); Table S1). The Hi-C data were first combined with published genetic map information to assign scaffolds to chromosomes using a novel iterative approach which resulted in a large reduction of the size of the 'unknown' chromosome chr. 0 (from 22.5% to 4.4% of the total assembly). The scaffolds of the final v3.0 assembly were super-scaffolded with optical maps, introducing long stretches of N bases and considerably altering scaffold size and order. We applied Hi-C to the pre-optical map scaffold set, ultimately improving the order and significantly reducing the proportion of N bases (from 28.2% to 9.1%). Following Hi-C-based automated scaffold ordering and manual editing with the aid of Hi-C contact plots, Hi-C asymmetry plots (Himmelbach *et al.*, 2018), and the positions of genetic map markers on the pseudomolecules, a near-optimal final order was found, which clearly improved the quality of the genome (Table 1; Figure S1(b)). Compared with v3.0, the percentage of anchored genes in v4.0 increased to 95.6% and the benchmarking against universal single-copy orthologs (BUSCO; Simão *et al.*, 2015) revealed 96.9% representation (Table 1). These values are comparable to those of the recent CL assembly (Wei *et al.*, 2020a). The size of individual chromosomes, which for some in our v3.0 was dissimilar from the one of the CL assembly, in v4.0 was highly comparable (Table S2). The CL and v4.0 assemblies exhibited high collinearity (Figure S2(a)), with just three minor intrachromosomal inversions in chrs. 2, 10, and 11. A comparison of the v4.0 and CL annotations showed a slight predominance of v4.0 proteins with similar lengths to those of their Arabidopsis homologs, as well as a slightly lower fraction of v4.0 proteins with no hit in the Arabidopsis annotation (Figure S2(b)).

Pan-genome construction and presence/absence variants

In addition to the reference line '67/3', 25 additional accessions were chosen on the basis of their genotype, phenotype, and geographic distribution, being representative of approximately 3600 genotyped accessions from a worldwide collection (<http://www.g2p-sol.eu/G2P-SOL-gateway.html>), exhibiting very diverse morphology with respect to fruit shape, pigmentation, and presence of prickles

Table 1 Metrics of publicly available eggplant genome assemblies: Smel v1.0 from Hirakawa *et al.* (2014), *S. aethiopicum* from Song *et al.* (2019), Smel v3.0 from Barchi *et al.* (2019b), Smel CL from Wei *et al.* (2020a), and Smel v4.0 (this paper)

	Smel v1.0	<i>S. aethiopicum</i>	Smel v3.0	Smel CL	Smel v4.0
Size of assembly (Gb)	0.83	1.02	1.21	1.07	1.16
Contig N50 (kb)	14.3	25.2	678.7	5260	702.9
Scaffold N50 (Mb)	0.065	516.1	2.9	89.64	92.1
% Ns	4.75	–	28.23	0.38	9.10
% anchored	–	–	77.5%	92.7%	95.6%
Protein-coding genes	85 446	34 906	34 916	36 582	34 916
% anchored genes	0%	0%	81.4%	97.4%	96.6%
Annotated BUSCO genes	74.8%	77.8%	96.9%	94.2%	96.9%

(Figure 1; Table S3). Resequencing data for nine of them were already available (Gramazio *et al.*, 2019), while the remaining 16 were subjected to paired-end (2×150 bp) Illumina sequencing, reaching an average coverage of 25-fold after cleaning, trimming, and removal of non-plant contaminants (Table S3). The genome for each accession was *de novo* assembled using Megahit into contigs larger than 500 bp. The final genome sizes ranged from 826 to 999 Mb and the N50 value from 3 to 26.8 kb (Table S3). All assembled contigs were compared to the reference genome to identify novel sequences. After removing redundancies,

these novel sequences were rechecked by removing contaminant sequences from non-green plants, resulting in the identification of approximately 51.5 Mb of additional sequences (available at <https://solgenomics.net/>).

A total of 816 protein-coding genes with Annotation Edit Distance (AED) score < 0.5 were predicted in the novel sequences using Maker-P. After Interproscan analysis, 439 novel genes contained at least a Pfam domain, and 631 contained Pfam or Panther domains. Overall, 365 new genes could be annotated with gene ontology (GO). The eggplant pan-genome, including reference and new

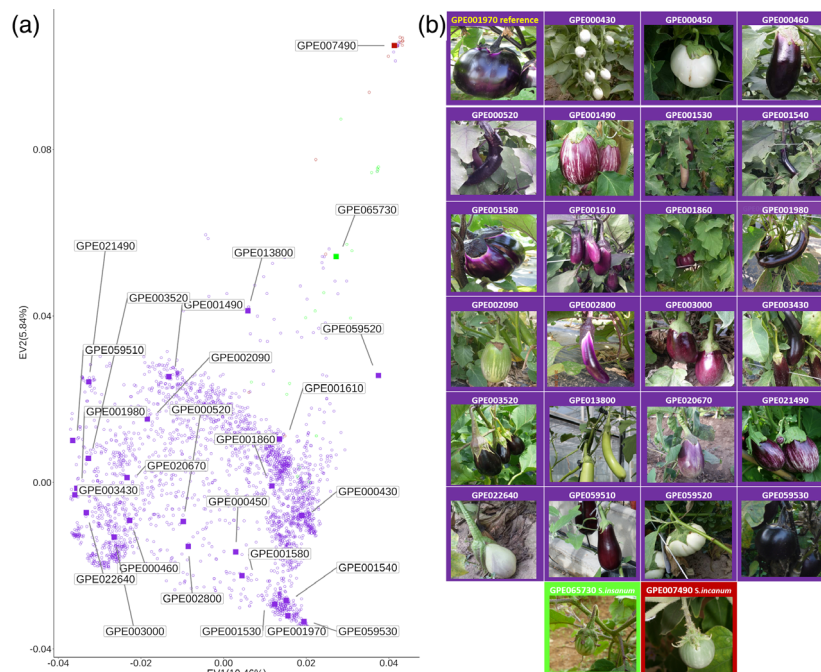


Figure 1. Accessions included in the eggplant pan-genome.

(a) PCA of 24 eggplant accessions from the G2P-SOL project, genotyped with a previously developed 5k SNP panel (Barchi *et al.*, 2019a). Resequenced accessions are depicted as squares. *Solanum melongena* entries are shown in purple, *S. insanum* entries in red, and *S. insanum* entries in green.

(b) Fruit phenotypes of the resequenced accessions.

genome sequences, had a total size of 1.21 Gbp and contained 35 732 protein-coding genes. A total of 41 non-reference genes were covered by reads of the reference line '67/3' with a coverage fraction greater than 95%, suggesting that they were not previously assembled in the reference genome. In total, 460 genes from the reference genome were not covered by reads in at least one of the accessions in this study (Table S4). Figure 2(a) shows how the pan-genome size was modeled by iterative random sampling of accessions. The model suggested an open pan-genome with a projected pan-genome size of 39 437 genes based on the Chao estimator (Chao, 1987). Indeed, the fitting of the curve in Figure 2(b) to a power law ($265.833n^{-0.59}$) indicates that adding another genome sequence would add 40 ± 4 additional genes (95% confidence interval) to the pan-genome.

The pan-genome genes were categorized based on their presence frequencies: 31 424 core genes were shared by all 26 accessions, 922 softcore genes were shared by 25 accessions, 1556 shell genes were shared by 2–24 accessions, and 1246 cloud genes were present just in one accession (Gao *et al.*, 2019; Gordon *et al.*, 2017) (Table S5). The core and softcore groups contained highly conserved genes, whereas the shell and cloud groups contained the so-called flexible genes. The reference genome v4.0 contained the majority of highly conserved genes (only 86 from the additional contigs) and around 78% of the flexible genes. Compared with the entire pan-genome, significant GO term enrichments were observed for the different pan-genome gene categories by using AGRIGO SEACOMPARE (Table S6). Several GO terms highly enriched in the flexible category were related to photosynthesis, protein synthesis (ribosome, structural constituent of ribosome, ribosomal subunit), and ATP biosynthetic processes. The flexible photosynthesis genes included several genes (*accD*, *petA*, *petB*, *ndhD*, *psaA-C*, *psbA-E*, *rbcL*, *ycf-2*)

probably resulting from differential organellar insertions in the nuclear genome of different accessions.

Pan-plastome construction and analysis

The complete chloroplast genomes of the 26 accessions were successfully assembled (Table S7) and submitted to GenBank (accession numbers MW384824–MW384851). They presented a typical quadripartite circular structure, composed of one long single copy (LSC) region, one short single copy (SSC) region, and two IRs (Figure 3(a)). In total, 79 protein-coding genes, 29–30 tRNA genes (with *trnG-UCC* present only in *S. incanum*), and 4 rRNA genes were identified (Table S8). Three pseudogenes (*infA*, *ycf1*, *rps19*) and 14 intron-containing genes (*rps16*, *atpF*, *rpoC1*, *ycf3*, *rps12*, *rpl2*, *clpP*, *ndhB*, *ndhA*, *trnA-UGC*, *trnI-GAU*, *trnK-UUU*, *trnL-UAA*, *trnV-UAC*) were also identified. The *rps12* gene was predicted to be trans-spliced, with the 5'-end located in the LSC region and the duplicated 3'-end in the IR region. The *trnK-UUU* had the largest intron, encompassing the *matK* gene, with 2513 bp, while the *trnI-GAU* had the shortest intron, with just 15 bp. Some genes were predicted to have an alternative start codon, like GTG (for *psbC* and *rps19*) or ATA (*petD*).

The aligned matrix of the 32 available plastomes (26 from this study and six from Aubriot *et al.* (2018)) was analyzed using DNAsp 6, resulting in the identification of 154 743 invariable and 449 variable sites, of which 186 were singletons and 263 were parsimony-informative. The total number of single-nucleotide polymorphisms (SNPs) in coding regions was 343.

The whole chloroplast genome sequences of all the accessions in the study were compared using the mVISTA program (Figure S3). The comparison revealed few differences in the *ycf1* gene and in the *trnA-trnR* intergenic region among the chloroplast genomes of the *S. melongena* accessions, with the exclusion of GPE001530. The number of

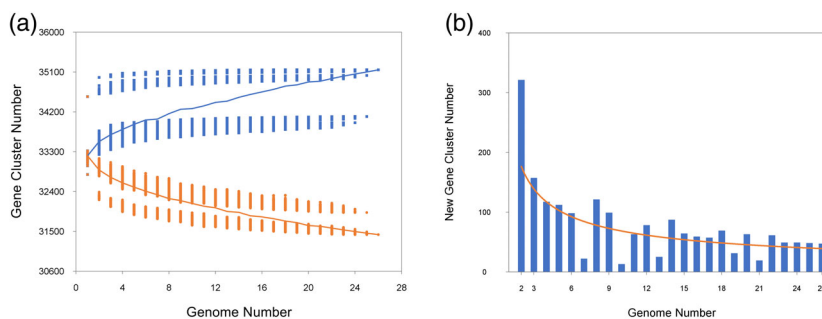


Figure 2. The eggplant pan-genome.

(a) Gene accumulation curves of the pan-genome (blue) and the core genome (orange). These curves describe the number of new genes (pan-genome) and genes in common (core genome) obtained by adding a new genome to a previous set. The blue vertical lines denote the pan-genome size for each genome for comparison. The orange vertical lines show the core genome size for each genome for comparison. The curve is the least squares fit of the power law for the average values.

(b) Curve (orange) for the number of new genes at each increase in the number of genomes.

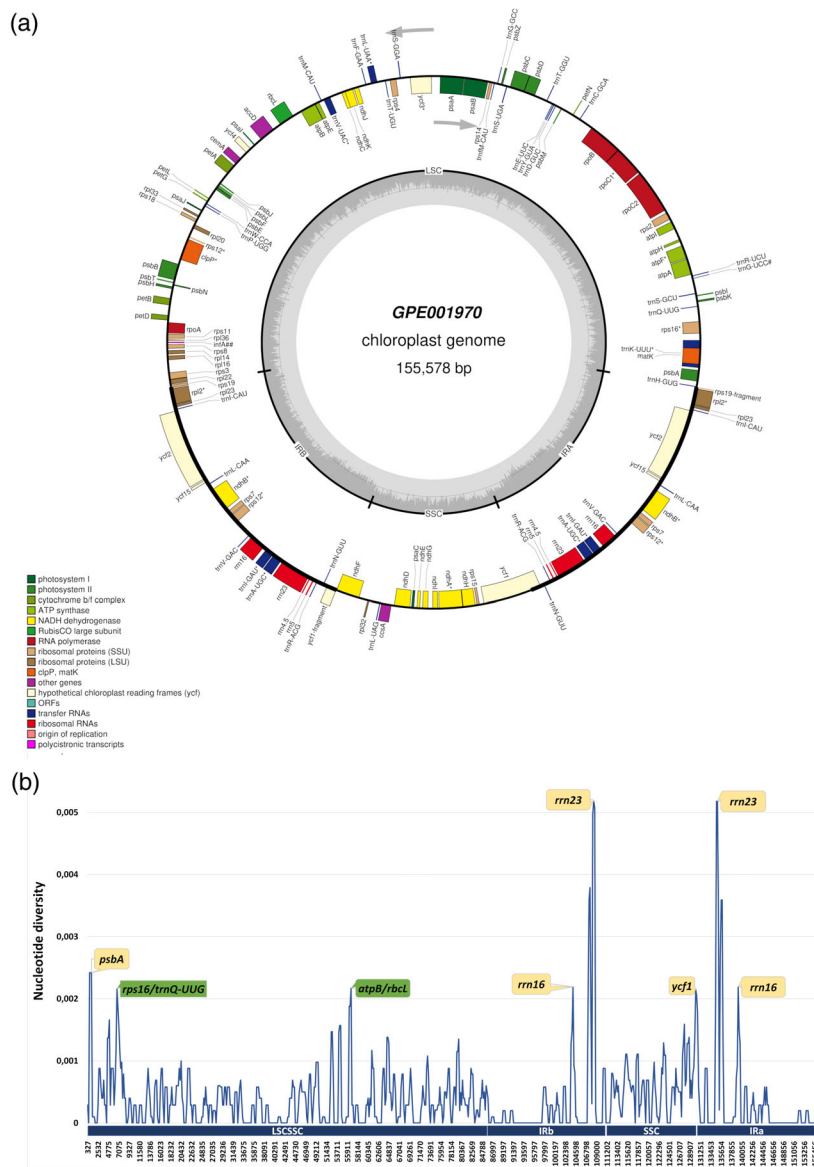


Figure 3. The eggplant pan-plastome. (a) Circular gene map of the chloroplast genome from the reference line GPE001970. Genes drawn inside the circle are transcribed clockwise, and those outside the circle are transcribed counterclockwise. The darker gray in the inner circle represents GC content. (b) Nucleotide diversity (P_i) values in the eggplant pan-plastome. Mutational hotspots with P_i values >0.002 in the intergenic spacers (IGSs) are shown in green, and those within genes are shown in yellow.

differences increased by extending the analyses to *S. insanum*, the species most similar to *S. melongena*, and to *S. incanum* (see intergenic regions *psaA-ycf3* and *rpl32-trnL* as examples). Expectedly, non-coding regions, in particular the intergenic spacers (IGSs), exhibited a higher divergence than coding regions.

The nucleotide variability (P_i) of the chloroplast genome was calculated (Figure 3(b)). The average value of P_i was relatively low (0.00039). The IR regions exhibited a lower variability ($P_i = 0.00036$) than LSC ($P_i = 0.00037$) and SSC

($P_i = 0.00060$) regions (Figure 3(b)). Five mutational hotspots with high P_i values (>0.002) were identified, involving IGSs as well as genes (*psbA*, *rrn16*, *rrn23*, *ycf1*).

A total of 2374 plastid simple sequence repeat (SSRs) were identified across the 32 *Solanum* accessions (Figure S4(a)), ranging from 60 for MH283713 to 66 for GPE059520 and GPE065730. The majority were mono-nucleotide (A/T), followed by di- and tri-nucleotide (AT/TA and AAT/ATT) repeats. By contrast, the tri-nucleotide motif AAC/GTT and the tetra-nucleotide AAAG/CTTT was only

found in one *S. incanum* chloroplast. The analysis of the 32 plastomes, using REPUTER, identified a total of 1174 repeats (30–79 bp) (Figure S4(b)). The proportions of repeats located in non-coding regions were higher than in coding regions, with *ycf2* showing the highest rearrangements.

Nuclear genetic diversity

The sequence reads of the 26 accessions (including the reference line '67/3') were aligned to the pan-genome sequence, yielding 1500464 SNPs/indels (final SNP dataset), with 246 391 in exons and 577665 in introns. In the reference line '67/3', 127 944 sites were heterozygous and 4322 indels were identified (Table S9). For the remaining accessions, the number of SNPs (including both homozygous and heterozygous) ranged from 97 913 for *S. melongena* GPE059530 to 6 047 125 for *S. incanum*, while the number of indels ranged from 4663 for *S. melongena* GPE059530 to 301172 for *S. incanum*.

Within the *S. melongena* accessions, the genomic residual heterozygosity was generally low, with the highest value being 0.04%. Of the two NMSs, *S. insanum* showed a higher level of homozygosity than *S. incanum*. The same trend was observed for the heterozygosity at the SNP/indel level, with *S. melongena* accessions showing no more than 5.46% of heterozygous sites compared to 22.30% of *S. insanum* and 34.33% of *S. incanum* (Table S9). The distribution of SNPs varied according to the species and the chromosomes (Figure S5; Table S10).

The maximum likelihood (ML) dendrograms based on the pan-genome and pan-plastome sequences (Figure 4(a)) grouped the accessions into two main branches. One branch includes all the *S. melongena* accessions together with their direct ancestor *S. insanum*, while a second branch includes *S. incanum*. *Solanum insanum* resulted closely related to two *S. melongena* accessions (GPE059520

and GPE000430) in both the nuclear and plastid phylogenies; both accessions are small-fruited and are characterized by low vigor and a semi-prostrate growth habit which is typical of some *S. insanum* accessions (Ranil *et al.*, 2017) although they, unlike *S. insanum*, have no or few prickles (Table S3).

The principal component analysis (PCA) based on the whole pan-genome SNP dataset (Figure S6(a)) largely confirmed the grouping of genotypes obtained in the ML-based dendrogram. The first and second principal components account, respectively, for 18.88% and 11.68% of the genetic variation. Eggplant accessions are clearly separated from NMSs by the first component of the PCA. By restricting the PCA to the 24 *S. melongena* accessions, a higher separation was obtained (Figure S6(b)), and the first and second principal axes accounted, respectively, for 14.76% and 9.66% of the genetic variation. Almost all accessions group together, with the exclusion of GPE001980.

Nucleotide diversity (π) was 0.000502 for the *S. melongena* accessions and 0.00204 for NMSs. Linkage disequilibrium (LD) decay in *S. melongena* accessions stabilized at about 0.41 at a distance of approximately 1.5 Mb (Figure S7), while in the whole panel of accessions, LD decay stabilized at about 0.35 at 1.4 Mb.

Phylogenetic analysis and PCA using the PAV matrix largely agree with what was previously observed based on the SNP information. The ML dendrogram (Figure 4(b)) identified two main branches; the first one included all the *S. melongena* accessions and the *S. insanum* accession, while *S. incanum* was assigned to the second one. In the PCA graph (Figure S6(c)), the first and second principal axes account for 17.47% and 13.92% of the genetic variation, respectively. The closest species to *S. melongena* accessions is its wild ancestor *S. insanum*. Again, by restricting the analysis to the 24 *S. melongena* accessions a clear separation among them was obtained (Figure S6(d)). GPE001970, the reference

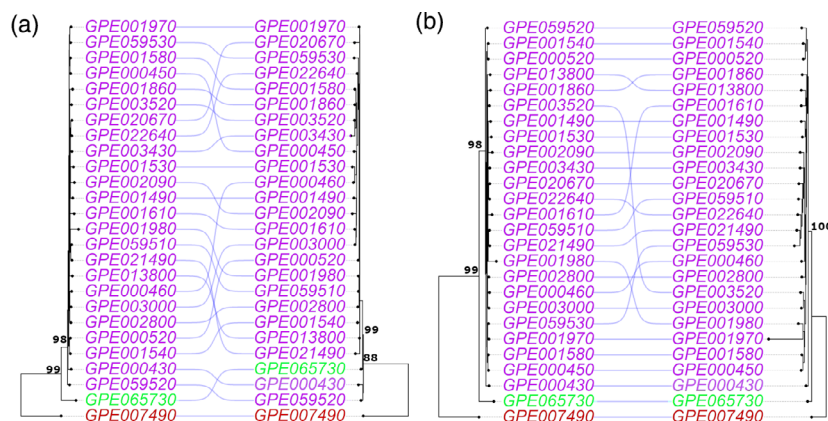


Figure 4. (a) Comparison of maximum likelihood phylogenetic trees, based on the nuclear (left) and plastidial (right) SNPs. (b) Comparison of maximum likelihood phylogenetic trees based on the nuclear SNPs (left) and PAVs (right). *Solanum melongena* entries are shown in purple, *S. incanum* entries in red, and *S. insanum* entries in green. Bootstrap values for main branches are also reported.

'67/3' line, shows a larger distance from the others in the PAV-based tree (Figure 5(b)) and PCA (Figure S6(d)). This is probably an artifact, due to the higher read coverage available following deeper sequencing of this accession (150-fold) with consequently around 1000 PAVs identified only in this accession.

Selective sweeps

The resequenced accessions show contrasting phenotypes for a series of phenotypic traits, such as fruit pigmentation

(FP), presence/absence of prickles (PR), and fruit shape (FS) (Figure 1; Table S3). Given the lack of noticeable population structure in the accessions (Figure 4), we decided to conduct a search for potential selection signatures by comparing the genomes of eggplant accessions contrasting for these traits. Five different comparisons were made: accessions with non-anthocyanic versus anthocyanic fruits (NAvsA), prickly versus non-prickly fruits (PvsNP), round versus long fruits (RvsL), round versus oval fruits (RvsO), and long versus oval fruits (LvsO). Two commonly used

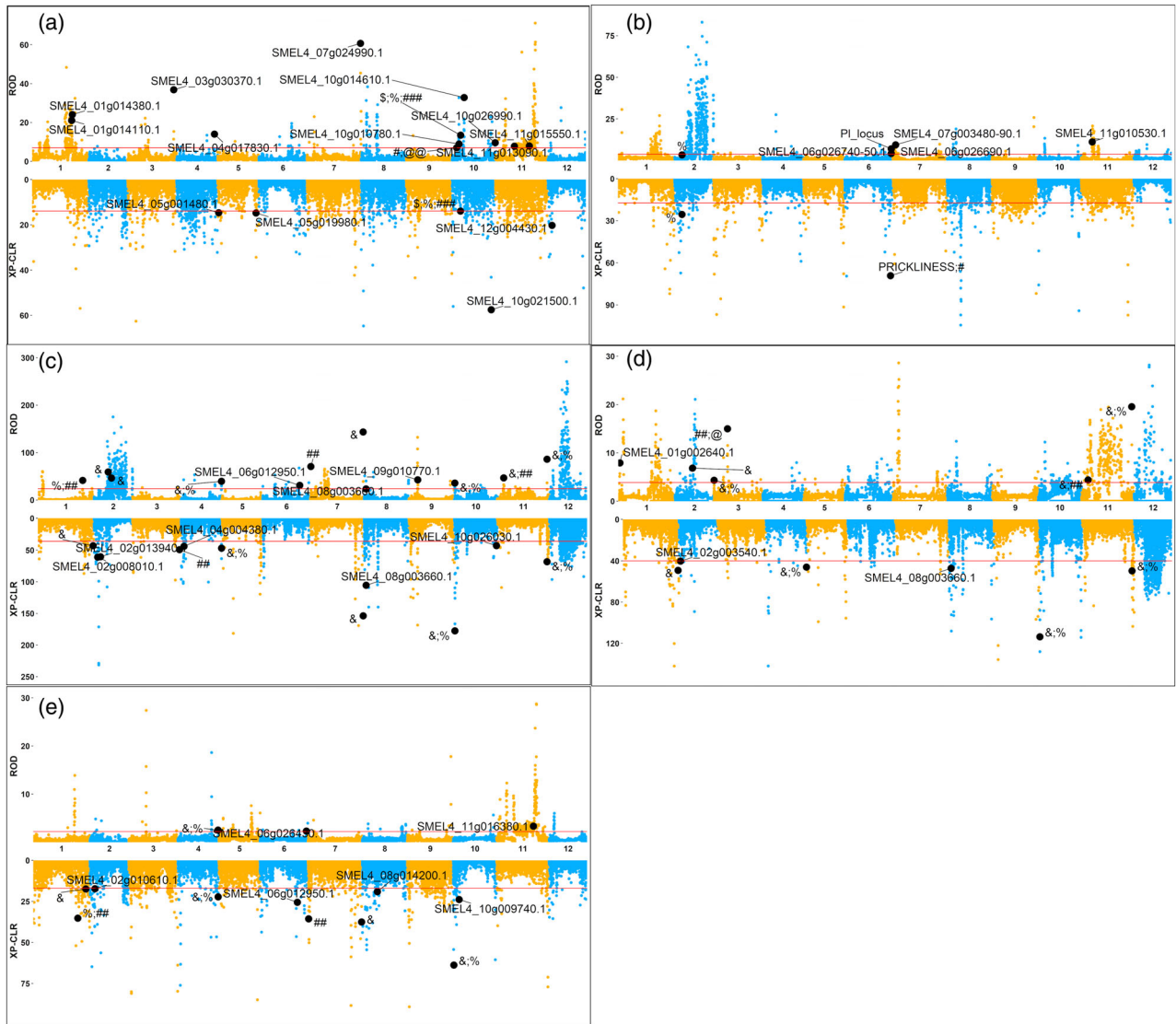


Figure 5. Plot of the π ratio (i.e., ROD; top) and XP-CLR (bottom) across the eggplant genome.

(a) Non-anthocyanic versus anthocyanic fruits (NAvsA).

(b) Prickly versus non-prickly fruits (PvsNP).

(c) Round versus long fruits (RvsL).

(d) Round versus oval fruits (RvsO).

(e) Long versus oval fruits (LvsO). The positions of previously discovered quantitative trait loci (QTLs) and quantitative trait nucleotides (QTNs) (\$Barchi *et al.*, 2012; ###Cericola *et al.*, 2014; &Portis *et al.*, 2014; #Frery *et al.*, 2014; %Portis *et al.*, 2015; @@Toppino *et al.*, 2016; ##Wei *et al.*, 2020b; @Wei *et al.*, 2020a; PI locus from Miyatake *et al.*, 2020) as well as candidate genes (Table 2) located in selective sweep regions are shown. Red lines represent cutoff values for the top 5% and 1% of ROD and XP-CLR scores, respectively.

indicators, the reduction in average nucleotide diversity (ROD or π ratio) and the cross-population composite likelihood ratio test (XP-CLR; Chen *et al.*, 2010) were used to identify selective sweeps (SSs), at cutoff values of 5% and 1%, respectively (Figure 5; Table S11). For each comparison, the SSs with top 5% ROD or 1% XP-CLR values covered, on average, 1458 (4.17%) and 1014 (2.90%) genes, respectively (Table S12).

We also searched for previously detected QTLs and/or quantitative trait nucleotides (QTNs) (Barchi *et al.*, 2012; Cericola *et al.*, 2014; Frary *et al.*, 2014; Portis *et al.*, 2014; Portis *et al.*, 2015; Toppino *et al.*, 2016; Wei *et al.*, 2020b) (Figure 5). We also searched for candidate genes putatively involved in the control of the examined phenotypic traits, mapping in the SSs regions (Table 2); this resulted in the identification of 53 SSs spanning 35.3 Mb (Figure 5). No PAVs putatively involved in the control of the traits in study were found to map to any of the SS regions identified.

Several candidate genes encoding proteins potentially involved in fruit anthocyanin pigmentation were identified in the SS regions (Figure 5; Table 2), including homologs of biosynthetic genes (*FLAVONOL SYNTHASE [FLS]*, *CHALCONE ISOMERASE [CHI]*, *ANTHOCYANIDIN REDUCTASE [ANR]*, *DIHYDROFLAVONOL 4-REDUCTASE [FRR]*) and genes encoding multidrug and toxin extrusion (MATE) and ATP-binding cassette (ABC) transporters mediating anthocyanin sequestration in other species (Francisco *et al.*, 2013; Jaakola *et al.*, 2002; Pérez-Díaz *et al.*, 2014). Candidate genes also included homologs of *Prx31*, which encodes a peroxidase involved in anthocyanin degradation (Movahed *et al.*, 2016), and of genes encoding transcription factors involved in anthocyanin/proanthocyanidin regulation, such as *MYB14* (Hancock *et al.*, 2012) and *Sme1MYBL1* (Moglia *et al.*, 2020). Several QTLs and QTNs controlling fruit anthocyanin pigmentation co-localized with the SS on chr. 10 (Figure 5).

Genes encoding transcription factors putatively involved in trichome/prickle formation were spotted within the SS regions identified for this trait, including homologs of the Arabidopsis *GLABRA1 (GL1)* and *GLABROUS INFLORESCENCE STEMS2 (GIS2)* genes (Figure 5; Table 2). QTNs for fruit calyx and stem prickles map on SSs located on chrs. 2, 6, and 8, as well as the *PRICKLINESS* marker (Gramazio *et al.*, 2014) and the recently identified *PI* locus (Miyatake *et al.*, 2020), both falling within a SS on chr. 6 (Figure 5).

Several homologs of genes controlling fruit size/shape in tomato were identified in SS regions involved in fruit shape, including *FW2.2*, *YABBY/FASCIATED (FAS)*, *LOCULE NUMBER (LC)/WUSCHEL* (Muños *et al.*, 2011), *OVATE*, *IQ-domain/SUN (IQD)*, *SUPPRESSOR OF OVATE (SOV)*, and *CELL SIZE REGULATOR (CSR)*; Mu *et al.*, 2017) (Figure 5; Table 2). QTNs and QTLs previously identified on several chromosomes and controlling, among others, fruit shape, length, and diameter (on chrs. 1, 2, 3, 4, 7, 10,

11, and 12), weight (on chrs. 1, 2, 3, 10, 11, and 12), and yield (on chrs. 2 and 3) were syntenic to the identified SS regions (Figure 5).

DISCUSSION

Hi-C retrofitting of an eggplant short read assembly

The precipitous development of next-generation sequencing technologies has increased the numbers of novel genome assemblies deposited each year in public databases enormously. Presently, 10 277 draft eukaryotic genome assemblies are listed in the NCBI GenBank database, the vast majority of which are based on short read technologies. Recently, CL assemblies, based on a combination of short and long reads, optical mapping, 10× Genomics, and Hi-C scaffolding, have started to emerge. This is the case for eggplant, for which a short read- and optical mapping-based chromosome-anchored assembly (v3.0) was released in 2019 (Barchi *et al.*, 2019b), and a CL assembly, based on a combination of Illumina, Nanopore, 10× Genomics, and Hi-C scaffolding, was released in 2020 (Wei *et al.*, 2020a).

Through the simple scaffolding of the v3.0 assembly using chromosome conformation capture (Hi-C), we have increased its quality to a level comparable to that of the CL assembly in terms of contiguity, the fraction of Ns, and numbers of anchored and positioned genes. Up to 1.11 Gb of sequences, containing 96.4% of the predicted genes, have been anchored to the 12 chromosomes, and the size of chr. 0 (i.e., the unanchored sequences) has been reduced to just approximately 51 Mb, smaller than the one of the CL assembly. BlastP comparison with the Arabidopsis proteome and BUSCO analysis revealed that the quality of the v3.0/v4.0 annotation is comparable, or better than, that of the CL one, apart from tandemly repeated genes (e.g., NBS genes) and repetitive elements, which are probably underrepresented in v4.0. Thus, the methods developed here can be used for the inexpensive retrofitting of thousands of short read-based genome assemblies without having to rerun the corresponding annotations, which have been used for a long time and were often manually improved by the respective scientific communities.

An eggplant pan-genome and pan-plastome

A pan-genome represents the entire gene set for a species and includes core genes, present in all individuals, as well as genes absent in one or more individuals (Golicz *et al.*, 2016). We constructed an eggplant pan-genome of 26 accessions, of which 24 were of the cultivated *S. melongena* and one each from two closely related wild species (*S. insanum* and *S. incanum*). About 52 Mb of additional sequences were captured, including 816 protein-coding genes. These values are lower than those of other Solanaceae pan-genomes containing a much larger number of resequenced accessions, for example, 351 Mb and 4873

Table 2 Selected candidate genes identified within selective sweep regions for the traits studied

Trait	Gene ID	ROD	XPCLR	Annotation	Note
		5%	1%		
Fruit pigmentation	SMEL4_01g014380.1	Yes	No	ABCC4: ABC transporter C family member 4	Homolog of <i>Vitis</i> ABCC1
	SMEL4_01g014110.1	Yes	No	PER64: Peroxidase 64	Homolog of <i>Vitis</i> Peroxidase 31
	SMEL4_01g014400.1	Yes	No	ABCC4: ABC transporter C family member 4	Homolog of <i>Vitis</i> ABCC1
	SMEL4_03g030370.1	Yes	No	Flavonol synthase/flavanone 3-hydroxylase (Fragment)	Homolog of Arabidopsis FLS
	SMEL4_04g017830.1	Yes	No	PER9: Peroxidase 9	Homolog of <i>Vitis</i> Peroxidase 31
	SMEL4_05g001480.1	No	Yes	CHI3: Probable chalcone–flavonone isomerase 3	Homolog to Arabidopsis CHI3
	SMEL4_05g019980.1	No	Yes	PER46: Peroxidase 46	Homolog of <i>Vitis</i> Peroxidase 31
	SMEL4_07g024990.1	Yes	No	ABCC3: ABC transporter C family member 3	Homolog of <i>Vitis</i> ABCC1
	SMEL4_10g010780.1	Yes	No	CHI: Chalcone–flavonone isomerase	Homolog of petunia CHI
	SMEL4_10g014610.1	Yes	No	MYB14: Transcription factor MYB14	Homolog of <i>Medicago</i> MYB14
	SMEL4_10g021500.1	No	Yes	DTX21: Protein DETOXIFICATION 21	Homolog of <i>Vitis</i> MATE1
	SMEL4_11g013090.1	Yes	No	Putative anthocyanidin reductase	Homolog of <i>Vitis</i> ANR
	SMEL4_11g015550.1	Yes	No	DFR1: Dihydroflavonol 4-reductase (fragment)	Homolog of <i>Medicago</i> DFR
	SMEL4_10g010780.1	Yes	No	CHI: Chalcone–flavonone isomerase	Ortholog of Arabidopsis TT5
	SMEL4_10g026990.1	Yes	No	MYB4: Transcription repressor MYB4 (AtMYBL2)	Eggplant MYBL1
	Prickliness	SMEL4_12g004430.1	No	Yes	DTX29: Protein DETOXIFICATION 29
SMEL4_06g026690.1		Yes	No	NUDT19: Nudix hydrolase 19 chloroplastic	<i>PI</i> locus
SMEL4_06g026740.1		Yes	No	GATA11: GATA transcription factor 11	<i>PI</i> locus
SMEL4_06g026750.1		Yes	No	ARF18: Auxin response factor 18	<i>PI</i> locus
SMEL4_07g003480.1		Yes	No	MYB82: Transcription factor MYB82	Homolog of Arabidopsis GI1
SMEL4_07g003490.1		Yes	No	MYB82: Transcription factor MYB82	Homolog of Arabidopsis GI1
Fruit shape	SMEL4_11g010530.1	Yes	No	GIS2: Zinc finger protein GIS2	Homolog of Arabidopsis GLS2
	SMEL4_01g002640.1	Yes	No	PCR2: Protein PLANT CADMIUM RESISTANCE 2	Homolog of tomato FW2.2
	SMEL4_02g003540.1	No	Yes	CNR1: Cell number regulator 1	Ortholog of tomato FW2.2
	SMEL4_02g008010.1	No	Yes	OPF7: Transcription repressor OPF7	Ortholog to tomato ovate
	SMEL4_02g010610.1	No	Yes	WUS: Protein WUSCHEL	Ortholog of tomato LC/WUS
	SMEL4_02g013940.1	No	Yes	PCR1: Protein PLANT CADMIUM RESISTANCE 1	Homolog of tomato FW2.2
	SMEL4_02g015770.1	No	Yes	WOX9: WUSCHEL-related homeobox 9	Homolog of tomato LC/WUS
	SMEL4_02g015780.1	No	Yes	WOX8: WUSCHEL-related homeobox 8	Homolog of tomato LC/WUS
	SMEL4_04g004380.1	No	Yes	IQD1: Protein IQ-DOMAIN 1	Homolog of tomato SUN
	SMEL4_06g012950.1	No	Yes	IQD14: Protein IQ-DOMAIN 14	Homolog of tomato SUN
	SMEL4_06g026430.1	Yes	No	YAB2: Putative axial regulator YABBY 2	Homolog of tomato FAS
	SMEL4_08g003660.1	Yes	Yes	YAB4: Protein YABBY 4	Homolog of tomato FAS
	SMEL4_08g014200.1	No	Yes	IQD1: Protein IQ-DOMAIN 1	Homolog of tomato SUN
	SMEL4_09g010770.1	Yes	No	FAF3: Protein FANTASTIC FOUR 3	Homolog of tomato CSR
	SMEL4_10g009740.1	No	Yes	OPF2: Transcription repressor OPF2	Ortholog of tomato suppressor of ovate
	SMEL4_10g026030.1	No	Yes	PCR12: Protein PLANT CADMIUM RESISTANCE 9	Homolog of tomato FW2.2
	SMEL4_11g016380.1	Yes	No	IQD1: Protein IQ-DOMAIN 1	Homolog of tomato SUN

genes in 725 tomato accessions (Gao *et al.*, 2019); and 956 Mb and 6984 genes in 383 pepper accessions (Ou *et al.*, 2018). The eggplant pan-genome contains >88% of core genes, similar to *Brassica oleracea* (Golicz *et al.*, 2016), but higher than tomato (74.2%; Gao *et al.*, 2019), Arabidopsis (70%; Contreras-Moreira *et al.*, 2017), and *Brassica napus* (62%; Hurgobin *et al.*, 2018). These differences are due to the genetic diversity of each taxon, as well as to the number of accessions and species included

in each pan-genome project. Based on the data shown here, we postulate a 400-accession pan-genome of *S. melongena* to contain up to 5249 additional genes with respect to the reference genome, with the 400th genome still providing eight new genes, while the core genome would be composed of 31 227 genes. This number of additional genes is slightly higher than the one predicted using the Chao estimator (4521), which gives a conservative estimate of pan-genome size.

The size of the chloroplast genome was similar to the ones reported for pepper, tomato, and potato (Kahlau *et al.*, 2006; Magdy *et al.*, 2019; Wu, 2016) and its sequence was highly conserved. However, few faster-evolving loci, namely *ycf1* and the intergenic region *trnA-trnR*, might be of use for DNA barcoding purposes (Hollingsworth *et al.*, 2009). A high level of conservation was also observed for GC content and gene numbers, which were similar to those of the other cultivated Solanaceae (Zhang *et al.*, 2018b). One tRNA (*trnG-UCC*) was complete in the *S. incanum* accession, suggesting a species-specific loss. The *ycf1* gene starts in the SSC region, but its sequence crosses the SSC/IRa boundary, causing a duplication of the 3'-end portion in IRb, thus producing a <1000-bp *ycf1* pseudogene, similar to what was observed in tomato, potato, and *Nicotiana* (Chung *et al.*, 2006). In addition to IRa extending into the *ycf1* gene, IRb also extends into the *rps19* gene, creating a duplication of various lengths of the 5'-end of the *rps19* gene at the IRa/LSC border. Only one copy of *rps19* is still functional, while the other turned into a pseudogene, as observed in other Solanaceae (Chung *et al.*, 2006). A similar situation is observed for *infA*, coding for translation initiation factor 1, which represents a classic example of chloroplast-to-nucleus gene transfer; it is a pseudogene in eggplant and in at least 17 other Solanaceae species examined, suggesting the gene was lost in the common ancestor of this family (Millen *et al.*, 2001).

Genetic diversity

The average heterozygosity in *S. melongena* accessions was less than 0.03%, slightly lower than previously reported (Barchi *et al.*, 2019a; Gramazio *et al.*, 2019), confirming the prevalent autogamy exhibited by the species. In the two NMSs (*S. insanum* and *S. incanum*), heterozygosity was on average higher (0.29%), consistent with their partial allogamy (Acquadro *et al.*, 2017; Daunay *et al.*, 2001b; Vorontsova and Knapp, 2016). Chromosome 2 was the richest in SNPs, probably reflecting the inclusion among the *S. melongena* accessions of the breeding line '305E40' (GPE001980), carrying a large introgression from *S. aethiopicum* in chr. 2 (Portis *et al.*, 2014; Toppino *et al.*, 2008).

Based on the whole SNP dataset, *S. melongena* accessions clustered separately from the NMS accessions, in both the ML dendrogram and the PCA graph. The ML tree based on the PAV matrix provided similar results, with *S. insanum*, the direct wild ancestor of *S. melongena* (Knapp *et al.*, 2013), showing a similar separation from eggplant accessions. On the other side, the tree we constructed on the basis of the chloroplast genome sequences was sufficient to correctly separate eggplant from *S. incanum*, while *S. insanum* is more closely related to two *S. melongena* accessions (GPE059520 and GPE000430) which are

small-fruited, have low vigor, and exhibit semi-prostrate growth.

Selective sweeps and domestication

Several previous studies highlighted a decrease of genetic diversity in domesticated species compared to their wild relatives (Bellucci *et al.*, 2014; Gao *et al.*, 2019; Liu *et al.*, 2019), especially in autogamous species. Although only one *S. insanum* (the direct progenitor of *S. melongena*) and one *S. incanum* (a close relative) accession were used in the analysis, the nucleotide diversity (π) for *S. melongena* suggests that the cultivated species underwent a reduction in diversity ($\pi_{insinc}/\pi_{eggplant} = 4.06$), attributable to genetic bottlenecks during domestication. This is in line with a recent estimate of a 47% loss of genetic diversity following domestication in the species (Page *et al.*, 2019).

Several SSs related to different phenotypic traits were identified (Tables S11 and S12). The stringent criteria used (top 5% ROD and/or top 1% XP-CLR) allowed to narrow down the numbers of candidate genes falling within SSs for each trait. On average, for each scored trait, the SSs defined by either of the two criteria comprised 2400 (6.87%) genes, while those defined by both criteria comprised 276 (0.79%) genes. Although the exact locus targeted by selection cannot be determined from sweep data alone, the overlap between QTLs, QTNs, and candidate genes from previous studies and SSs is suggestive of which traits have been shaped by positive selection during eggplant evolution, and in some cases can be tied to known candidate genes. The absence of PAVs within SSs for the traits under study suggests that breeding for these traits acted by selecting for allelic variants, rather than by introducing or deleting individual genes.

Anthocyanin biosynthesis is one of the most studied pathways in plants. Its control is strongly dependent on the tissue, developmental stage, and environment, and has been partially elucidated in eggplant (Barchi *et al.*, 2019b; Moglia *et al.*, 2020; Xiao *et al.*, 2018; Zhang *et al.*, 2014). Modern eggplant varieties present anthocyanin pigmentation of the peel, whereas ancestral genotypes present non-anthocyanic (white or green) fruits. By comparing genotypes with white/green versus purple fruits, a SS on chr. 10 was identified, which contains the transcriptional repressor gene *SmelMYBL1* (Moglia *et al.*, 2020) as well as QTLs and QTNs for flower color and anthocyanin accumulation (Barchi *et al.*, 2012; Cericola *et al.*, 2014; Fray *et al.*, 2014; Portis *et al.*, 2015; Toppino *et al.*, 2016). *SmelMYBL1* encodes an R3 MYB transcription factor and represents a novel component of the eggplant bHLH, MYB, WD40 (BMW) regulatory complex, where it probably competes with MYB activators of anthocyanin gene transcription (*SmelANT1* and *SmelAN2*). Other candidate genes localized on different chromosomes include homologs of anthocyanin biosynthetic genes (*ANR*, *FLS*, *CHI*, *FRR*) and

ABC transporters mediating vacuolar transport of anthocyanins in *Vitis vinifera* (Francisco *et al.*, 2013). In addition, homologs of *V. vinifera Prx31*, which encodes a peroxidase involved in anthocyanin degradation (Movahed *et al.*, 2016), and *MATE1*, encoding proanthocyanidin transporter (Pérez-Díaz *et al.*, 2014), as well as a gene encoding an R2R3-MYB transcription factor (MYB14) involved in the regulation of proanthocyanidins in legumes (Hancock *et al.*, 2012). Prickles are a distinctive trait of eggplant and its wild relatives, the *Solanum* subgenus *Leptostemonum* (spiny solanums) comprising approximately 450 species (Knapp *et al.*, 2019). Although prickly eggplant types are preferred in certain regions on the basis of their perceived superior organoleptic quality, prickles are generally considered an undesirable trait and they have been counter-selected in several modern varieties (Daunay *et al.*, 2001a). It is thought that plant prickles are modified glandular trichomes and that their biogenesis is controlled by transcription factors from the MYB, bHLH, WD40, WRKY, and C2H2 zinc finger families (Wang *et al.*, 2019). Indeed, by comparing prickled and non-prickled genotypes, we identified several SSs containing genes encoding homologs of Arabidopsis transcription factors involved in trichome initiation, such as *GL1* and *GIS2* (Wang *et al.*, 2019; Zhang *et al.*, 2021). SSs on chr. 6 fall in proximity of previously identified QTLs and QTNs as well as the morphological marker PRICKLINESS (Frary *et al.*, 2014; Gramazio *et al.*, 2014; Portis *et al.*, 2015) and the recently identified *PI* locus involved in prickle formation in eggplant (Miyatake *et al.*, 2020; Zhang *et al.*, 2021), suggesting that these regions have been the targets of human selection for presence/absence of prickles.

Fruit size and shape are key traits for breeding and are controlled by several genes. In tomato, genes controlling fruit size and shape include *CELL SIZE REGULATOR (CSR)*, *FW2.2*, *KLUH/FW3.2*, *OVATE FAMILY PROTEIN (OFP)*, *SOV*, *TONNEAU RECRUITING MOTIF (TRM5)*, *SUN/IQD*, *LC/WUSCHEL*, and *FAS/YABBY* (reviewed in van der Knaap and Østergaard, 2018). Fruit shape SSs in the resequenced accessions contain several homologs of *CSR*, *FW2.2*, *OVATE*, *SOV*, *SUN/IQD*, *LC/WUSCHEL*, and *FAS/YABBY*. In particular, the eggplant orthologs of *FW2.2*, *OVATE*, *LC/WUSCHEL*, *SOV*, and *CSR* are localized in SSs for fruit shape on chrs. 2, 10, and 12. *LC*, together with *FAS*, controls locule number and, consequently, flat shape in tomato. *LC* and *FAS* mutations arose early during tomato domestication, and contributed to the man-made selection for increased fruit size (van der Knaap and Østergaard, 2018; Muñoz *et al.*, 2011; Rodríguez *et al.*, 2011). Our data suggest that selection involving eggplant *LC* occurred during the selection of modern large and more elongated fruit types from the original small and round-fruited ones. *CSR* encodes an uncharacterized protein whose clade has expanded in the Solanaceae family and the large-fruited allele is found in *S. lycopersicum*

var. *cerasiforme*, suggesting that the selection at this locus was critical to the early domestication of tomato (Mu *et al.*, 2017). Again, our data appear to confirm that selection at the eggplant ortholog had an influence on fruit shape. Additional QTLs and QTNs previously identified (Mangino *et al.*, 2021; Portis *et al.*, 2014, 2015; Wei *et al.*, 2020b) and controlling fruit shape and size, as well as a recently identified region controlling fruit length (Wei *et al.*, 2020a), fall within some of the SSs identified. However, we have not found, within the high-confidence SS intervals for fruit shape, any *SUN* gene homologs like the one reported by Wei *et al.* (2020a) on chr. 3. This might be due to the absence of alleles of this gene in our resequenced accessions, which do not include extremely elongated fruit shaped accessions like in the study of Wei *et al.* (2020a).

In conclusion, the improved assembly of the eggplant reference genome and the first eggplant pan-genome and pan-plastome described in this paper add depth and completeness to our genomic understanding of eggplant and its breeding history. The identification of SSs and candidate genes for key eggplant agronomic traits lays the foundations for an initial understanding of the genomic events underlying domestication and selection of this important vegetable species.

EXPERIMENTAL PROCEDURES

Generation of the v4.0 assembly

Hi-C library construction and sequencing was conducted in the '67/3' *S. melongena* accession (G2P-SOL code GPE001970) previously sequenced (Barchi *et al.*, 2019b), as reported earlier (Padmarasu *et al.*, 2019). Adapter trimming, quality control, and validation of Hi-C fragments were conducted as previously described (Mascher *et al.*, 2017) using the scripts as implemented in the TRITEX pipeline (Monat *et al.*, 2019).

Hi-C contact scores between 200 000-bp bins were produced via binning and normalization of the interbin contact scores as described by Hu *et al.* (2012), also implemented using the TRITEX pipeline (Monat *et al.*, 2019). Two sets of scaffolds produced in eggplant assembly v3.0 were used for producing the updated assembly (v4.0): (i) the Illumina scaffolds from v3.0 and (ii) the superscaffolds generated by the optical mapping, plus the Illumina scaffolds not incorporated into a superscaffold. Superscaffolds were given initial chromosome assignments using the mapped positions and linkage groups of the genetic map markers generated by Barchi *et al.* (2019a). For the set of markers mapped to a superscaffold, if the most commonly represented linkage group outnumbered the second most common by >2:1, then the v3.0 scaffolds comprising the superscaffold were initially assigned to the chromosome associated with that linkage group. We applied a three-phase process to optimize the chromosome assignments of the v3.0 scaffolds:

- i 'Capture' phase: Hi-C links between chromosome-assigned and unassigned scaffolds were tabulated, and unassigned scaffolds were assigned to a chromosome if (1) there were at least five Hi-C links involving the scaffold and other chromosome-assigned scaffolds and (2) the number of links

joining to scaffolds assigned to the most commonly linked chromosome was at least 0.6 times the number of links to the next most commonly linked chromosome.

- ii 'Correction' phase: The assignments of all scaffolds were tested for consistency with the Hi-C information. Every scaffold's assignment was tested in the same way as during the capture phase, as though it was unassigned.
- iii 'Agreement' phase: Scaffolds were tested to check for disagreements between the Hi-C-based assignments and the original, map-based assignments. Scaffolds with more than three genetic map markers and for which the Hi-C-based and the map-based chromosome assignments disagreed were selected in order to remove their chromosome assignments.

The scaffolds were arranged into a tentative initial pseudo-molecule scaffold arrangement for each chromosome (known as 'A Golden Path' [AGP]) using the Burton *et al.* (2013) method as implemented in the TRITEX pipeline and by exploiting the homologous AGP positions of genetic map markers available from several publicly available eggplant genetic mapping studies (Fukuoka *et al.*, 2012; Hirakawa *et al.*, 2014; Miyatake *et al.*, 2012; Nunome *et al.*, 2009). Manual editing of the order then proceeded in 10 rounds by informed trial-and-error, until a near-optimal AGP was found, as revealed by visual inspection of the Hi-C contact matrices (Figure 1), Hi-C asymmetry plots (Himmelbach *et al.*, 2018), and aligned genetic map marker positions. Genome annotation was lifted from v3.0 to v4.0 using flo (Pracana *et al.*, 2017, Table S13).

For comparative purposes, v4.0 assembly was aligned against the CL assembly using minimap2 (Li, 2018) and plotted with dot-Plotly (<https://github.com/tpoorten/dotPlotly>). Finally, our proteome (34 916 proteins) and the one recently released (36 568 proteins; Wei *et al.*, 2020a), alongside those of tomato (ITAG4.1, 34 688 proteins), potato (ITAG v1, 35 004 proteins; The Tomato Genome Consortium, 2012), pepper (PGA v2, 35 884 proteins Kim *et al.*, 2017) and the eggplant annotation generated in Hirakawa *et al.* (2014) (Sme_r2.5.1, 42 035 proteins), were compared against the high-quality Arabidopsis nuclear proteome (TAIR10, 27 206 proteins; Lamesch *et al.*, 2012, p. 10) by BlastP (e-value = 10^{-3}), and the relative length ratios of the best protein pairs were computed.

Resequencing, assembly, and pan-genome/pan-plastome construction and annotation

Published genome sequencing data of nine *S. melongena* accessions and one *S. incanum* accession (Barchi *et al.*, 2019b; Gramazio *et al.*, 2019) were retrieved from the NCBI Sequence Read Archive (SRA) database. Genome sequences of a total of 16 additional genotypes available from a worldwide collection (<http://www.g2p-sol.eu/G2P-SOL-gateway.html>) and including 15 *S. melongena* genotypes and one *S. insanum* genotype were generated here. Genomic DNA was extracted from a single seedling from each of these 16 accessions using a Qiagen plant Mini-Prep kit. Paired-end libraries with insert sizes of approximately 350 bp were constructed using the NEBNext DNA Library Prep kit (Illumina Inc.) according to the manufacturer's instructions and sequenced on an Illumina Novaseq platform using the paired-end 2x150 bp mode. The sequencing raw data of the 16 newly sequenced accessions are available at NCBI SRA (BioProject ID PRJNA649091).

Adapters and low-quality sequences were trimmed from raw Illumina reads using Scythe (v0.994, <https://github.com/vsbuffalo/scythe>) to filter out contaminant substrings, and Sickle (v1.33, <https://github.com/najoshi/sickle>) was used to remove reads with poor-quality ends. Reads were error-corrected using the Spades

tool (v3.13) (Bankevich *et al.*, 2012). Finally, kraken2 (Wood *et al.*, 2019) was used to remove contaminant reads from bacterial, archaeal, and viral genomes (MiniKraken DB_8GB) as well as from fungi (complete fungi sequences, <https://www.ncbi.nlm.nih.gov/refseq/>).

High-quality cleaned Illumina reads from 25 samples (with the exclusion of the reference line) were *de novo* assembled using Megahit (v1.2.9) (Li *et al.*, 2015) with default parameters. The assembled contigs with lengths of >500 bp were kept and then aligned to the eggplant v4.0 genome of the line '67/3' using minimap2 (v2.17-r954-dirty) (Li, 2018) with setting 'asm10' for *S. melongena* and 'asm20' for other species. Contigs with no reliable alignments were kept as unaligned contigs. For contigs containing the reliable alignments, if they also contained continuous unaligned regions longer than 500 bp, the unaligned regions were extracted as unaligned sequences. The cleaned non-reference sequences from all accessions were combined. The redundant sequences were consolidated into unique contigs using CD-HIT (v4.8.1) (Fu *et al.*, 2012) and the non-redundant contigs were finally searched against the GenBank nucleotide database using BlastN (Camacho *et al.*, 2009). Sequences with best hits from outside the green plants or covered by known plant mitochondrial or chloroplast genomes were possible contaminations and hence were removed.

The final non-redundant non-reference sequences and the v4.0 assembly were merged into an eggplant pan-genome. Curve fitting of the pan-genome was performed using a power-law regression based on Heaps' law ($y = A_{\text{pan}}x^{B_{\text{pan}}} + C_{\text{pan}}$), where y is the pan-genome size, x the genome number, and A_{pan} , B_{pan} , and C_{pan} the fitting parameters, as previously described (Rasko *et al.*, 2008; Tettelin *et al.*, 2005, 2008). Fitting was conducted with PanGP software (Zhao *et al.*, 2014). B_{pan} was equivalent to the γ -parameter used by Tettelin *et al.* (2005, 2008) in estimating an open or closed pan-genome. When $0 < B_{\text{pan}} < 1$, the size of the pan-genome increases unboundedly with sequential additions of new genomes, thus indicating an open pan-genome. Conversely, when $B_{\text{pan}} < 0$ or $B_{\text{pan}} > 1$, the trajectory approaches a plateau as further genomes are added, indicating a closed pan-genome. Curve fitting of the core genome was performed using an exponential regression model ($y = A_{\text{core}}e^{(B_{\text{core}}x)} + C_{\text{core}}$), where y is the core genome size, x the genome number, and A_{core} , B_{core} , and C_{core} the fitting parameters. Estimation of pan-genome features was done using micropan (Snipen and Liland, 2015).

A custom repeat library was constructed and used to annotate the novel genome sequences using MAKER-P (v3.01.01) (Campbell *et al.*, 2014) with Augustus (v3.3.2) (Stanke *et al.*, 2006) and SNAP (version 2006-07-28) (Bromberg and Rost, 2007). The gene models identified with an AED of <0.5 were checked using InterProScan 5 (v. 5.44-79.0) (Jones *et al.*, 2014). Genes were functionally annotated by comparing their protein sequences against the SwissProt Viridiplantae database (The UniProt Consortium, 2014) and the InterPro domain database. GO enrichment was calculated using AGRIGO V2 (Tian *et al.*, 2017) as well as with AGRIGO cross-comparison of SEA (SEACOMPARE) to identify common and unique GO enrichment terms.

SNP calling, variant annotation, polymorphism estimates, LD decay, PAVs, and selective sweeps

The sequences were mapped to the pan-genome using the Burrows-Wheeler Aligner (BWA) program (v. 0.7.17-r1188) and the 'mem' command with default parameters (Li, 2013). BAM files were processed and used for the SNP calling using bcftools mpileup/call/norm utilities (v. 1.10.2) (Li, 2011) with default

parameters except for the use of the multi-allelic calling model ($-m$ option), minimum mapping quality ($Q = 20$), and filtering out multimapping events ($-q > 1$). Bcftools was applied to generate the final SNP dataset using a read depth of 10 as a cutoff and a max missing rate of 30% for retaining a SNP at the genotype level.

SNPs/indels were counted and analyzed using bcftools. The estimation of the heterozygous level of each genome (i.e., 'genome level') was calculated by considering, for each accession, the ratio between the number of SNPs/indels (called heterozygous state) and the ungapped size of the pan-genome, deprived of Ns (1.17 Gb) as previously reported (Acquadro *et al.*, 2020). Vcftools (Danecek *et al.*, 2011) was applied to count the number of SNPs along the reference genome using a sliding window approach (1-Mb windows, sliding in 500-kb steps). The results were plotted with R v4.0.3 (R Core Team, 2020).

RAxML-NG (v.0.9) (Kozlov *et al.*, 2019) was used to construct an ML tree and branch supports were obtained with an MRE-based bootstrapping test (Pattengale *et al.*, 2010). A PCA using the final SNP dataset was obtained with the SNPrelate (Zheng *et al.*, 2012) program; SNPs with a minor allele frequency (MAF) of < 0.05 were excluded. LD plots were calculated with PopLDdecay (Zhang *et al.*, 2018a), while Vcftools was used to calculate genetic diversity (π) and population differentiation (F_{ST}), which was estimated using Weir and Cockerham (Weir and Cockerham, 1984) values, using a sliding window approach (200-kb windows, sliding in 100-kb steps); SNPs with a MAF of < 0.05 were excluded.

SSs in *S. melongena* were identified for five contrasting fruit traits: (i) NAvsA; (ii) PvsNP; (iii) LvsO (length/width ratio > 2 versus length/width ratio = 1–2); (iv) RvsL (length/width ratio = approximately 1 versus length/width ratio > 2); and (v) RvsO (length/width ratio = approximately 1 versus length/width ratio = 1–2). Firstly, we calculated the ROD using a sliding window approach (200-kb windows, sliding in 100-kb steps; SNPs with a MAF of < 0.05 were excluded) in Vcftools between *S. melongena* accessions showing one of the five contrasting phenotypes in study. In parallel, an implementation (<https://github.com/hardingnj/xpclr>) of the XP-CLR (Chen *et al.*, 2010) was also used. For each chromosome, the XP-CLR score was calculated in 50-kb windows with parameters '--maxsnps 400, --rate 1e-8 --ld0 0.7'. Then, SS regions were identified as regions identified in the top 5% values for ROD statistics and/or in the top 1% of XP-CLR scores. Adjacent regions within the same phenotypic trait were merged with the bedtools suite (Quinlan and Hall, 2010).

Genome reads from each accession were aligned to the pan-genome using BWA-MEM (Li, 2013) with default parameters. The presence or absence of each gene in each accession was determined using SGSGeneLoss (v.0.1) (Golicz *et al.*, 2015). In brief, for a given gene in a given accession, if less than 20% of its exon regions were covered by at least two reads ($\text{minCov} = 2$, $\text{lostCutoff} = 0.2$), this gene was considered as absent in that accession; otherwise it was considered present. An ML phylogenetic tree was constructed based on the binary PAV data with 1000 bootstraps using IQ-TREE (Minh *et al.*, 2020). A co-phylogenetic plot of the ML dendrograms based on the pan-genome and PAV sequences was obtained using the R package phytools (Revell, 2012).

Chloroplast genome assembly and annotation

Chloroplast genomes of the resequenced accessions, together with the one from the *S. melongena* reference line '67/3', were assembled using GetOrganelle (Jin *et al.*, 2018) and annotated using GeSeq (Tillich *et al.*, 2017). The same annotation pipeline

was applied to already available eggplant chloroplast sequences, including those of three *S. melongena* (Aubriot *et al.*, 2018; Ding *et al.*, 2016), two *S. incanum*, and one *S. insanum* sequence from Aubriot *et al.* (2018). A circular plastome map representing *S. melongena* '67/3' lines was drawn using OrganellarGenome DRAW (Greiner *et al.*, 2019).

All plastomes were aligned using MAFFT v7 (Kato and Standley, 2013). A phylogenetic tree by the ML method using the IQ-TREE software (Nguyen *et al.*, 2015) was constructed; branch supports were obtained with the ultrafast bootstrap (Hoang *et al.*, 2018). A co-phylogenetic plot of the ML dendrograms based on the pan-genome and pan-plastome sequences was obtained using the R package phytools (Revell, 2012).

Hypervariable regions were identified with sliding window analysis in DNASP v6 (Rozas *et al.*, 2017). The mVISTA program (Frazer *et al.*, 2004) in Shuffle-LAGAN (Brudno *et al.*, 2003) mode was used to compare the cp genomes using '67/3' as a reference. The top 10 most variable non-coding regions of high Pi value were counted by potentially informative characters following Shaw *et al.* (2005).

The SciRoKo tool (Kofler *et al.*, 2007) was used to search for SSR loci (i.e., mono-, di-, tri-, tetra-, penta- and hexanucleotide repeats). The minimum numbers (thresholds) of repeats were 10, 5, 4, 3, 3, and 3 for mono-, di-, tri-, tetra-, penta-, and hexanucleotides, respectively. REPUTER (Kurtz *et al.*, 2001) was used to assess the number and location of repeat sequences, including direct (forward), inverted (palindromic), complement, and reverse repeats. For all the repeat types, the constraints set in REPUTER were (i) a minimum repeat size of 30 bp and (ii) 90% greater sequence identity with Hamming distance equal to 3 (i.e., the gap size between repeats had a maximum length of 3 bp). All overlapping repeats were removed from the final results.

ACKNOWLEDGMENTS

This work was supported by the European Commission, Horizon 2020 G2P-SOL project (grant agreement no. 677379). We gratefully acknowledge Ines Walde and Axel Himmelbach for technical assistance.

AUTHOR CONTRIBUTIONS

JP, SL, NS, GLR, and GG conceived the study. SP produced the Hi-C library. MTRW performed the genome assembly. LT provided materials. EP contributed producing sequencing data. LB produced and analyzed resequencing data. LB and GG wrote the manuscript. All authors critically revised and approved the manuscript.

CONFLICT OF INTEREST

The authors declare no conflict of interest.

DATA AVAILABILITY STATEMENT

All Raw Illumina data were deposited at NCBI SRA (BioProject ID PRJNA649091). The v4.0 and pan-genome assemblies and annotations are available at <https://solgenomics.net/>. Chloroplast genomes were submitted to GenBank (accession numbers MW384824–MW384851). Seeds of the accessions used in the present study can be obtained from COMAV (jprohens@btc.upv.es) or CREA (laura.topino@crea.gov.it).

SUPPORTING INFORMATION

Additional Supporting Information may be found in the online version of this article.

Figure S1. Hi-C scaffolding of the v3.0 eggplant genome assembly. (a) *In silico* inferred distribution of valid (valid restriction site-associated, religated) and invalid ('paired-end' [PE]) Hi-C fragment lengths in the Hi-C dataset (Monat *et al.*, 2019). (b) Hi-C contact frequency plots showing the improvement in chromosome-scale contiguity between assembly versions v3.0 (Barchi *et al.*, 2019) and v4.0 (current study). Log Hi-C link counts between 200-Mbp bins are given after normalization (see the Experimental Procedures section). Stark discontinuities in the contact frequencies are evidence of missing sequences or incorrectly arranged scaffolds.

Figure S2. (a) Synteny analysis of *S. melongena* '67/3' assembly v4.0 (on the x-axis) and the *S. melongena* CL assembly (y-axis). (b) Histogram of pairwise comparisons of predicted protein length ratios with their best hit in the Arabidopsis TAIR10 annotation (BlastP, e-value = 10^{-3}).

Figure S3. Comparison of 32 chloroplast genomes using mVISTA. Complete cp genomes were compared, with GPE001970 as a reference. Blue block: conserved genes, sky-blue block: tRNA and rRNA, red block: conserved non-coding sequences (CNSs). White represents regions with sequence variation.

Figure S4. Numbers of (a) SSRs and (b) repeats identified in the 32 chloroplast sequences. Colors depend on the motifs (a) or size (b) of the repeats identified.

Figure S5. Distribution of single-nucleotide polymorphisms (SNPs) along the reference genome sequence. The SNP distribution for all the accessions in the study is shown in orange, the SNP distribution only for eggplant is shown in purple, and the SNP distribution only for NMSs is shown in blue (*S. insanum* and *S. incanum*).

Figure S6. Principal component analysis (PCA) visualization of the genetic relationships among the accessions of eggplant as well as cultivated and wild related species, based on (a) the whole set of SNPs identified; (b) the whole set of SNPs identified limited to *S. melongena*; (c) PAVs; and (d) PAVs limited to *S. melongena*. *Solanum melongena* entries are shown in purple, *S. incanum* entries in red, and *S. insanum* entries in green.

Figure S7. Linkage disequilibrium (LD) decay in all accessions (orange) and *S. melongena* (purple). r^2 estimates were plotted against the physical distance.

Table S1. Hi-C metrics.

Table S2. Chromosome metrics of Smel v3.0 and v4.0 and their comparison with Smel CL.

Table S3. Phenotypic characteristics, geographical origin, and genome assembly metrics of the eggplant accessions.

Table S4. Pan-genome genes present or absent following read mapping in the reference line GPE001970 ('67/3').

Table S5. Different categories of genes in the eggplant pan-genome.

Table S6. Gene ontology (GO) term enrichments for different pan-genome gene categories using AGRIGO SEACOMPARE.

Table S7. Assembly metrics of the eggplant pan-plastome. The asterisk (*) indicates already assembled chloroplasts.

Table S8. List of genes in the eggplant pan-plastome.

Table S9. SNPs identified in the pan-genome sequences for all 26 accessions.

Table S10. SNP distribution per chromosome in the 26 accessions.

Table S11. Highest *ROD* and *XP-CLR* values for the 5 breeding traits in study in the selective sweeps identified.

Table S12. Selective sweeps number and size and genes number for the five breeding traits in study identified with *ROD* top 5% and/or *XP-CLR* top 1%.

Table S13. Conversion of gene models between annotations v3.0 and v4.0.

REFERENCES

- Acquadro, A., Barchi, L., Gramazio, P., Portis, E., Vilanova, S., Comino, C. *et al.* (2017) Coding SNPs analysis highlights genetic relationships and evolution pattern in eggplant complexes M. Singh, *ed.*, **12**, e0180774. <https://doi.org/10.1371/journal.pone.0180774>.
- Acquadro, A., Barchi, L., Portis, E., Nouridine, M., Carli, C., Monge, S. *et al.* (2020) Whole genome resequencing of four Italian sweet pepper landraces provides insights on sequence variation in genes of agronomic value. *Scientific Reports*, **10**, 9189. <https://doi.org/10.1038/s41598-020-66053-2>.
- Aubriot, X., Knapp, S., Syfert, M.M., Pocza, P. & Buerki, S. (2018) Shedding new light on the origin and spread of the brinjal eggplant (*Solanum melongena* L.) and its wild relatives. *American Journal of Botany*, **105**, 1175–1187. <https://doi.org/10.1002/ajb2.1133>.
- Bankevich, A., Nurk, S., Antipov, D., Gurevich, A.A., Dvorkin, M., Kulikov, A.S. *et al.* (2012) SPAdes: a new genome assembly algorithm and its applications to single-cell sequencing. *Journal of Computational Biology*, **19**, 455–477. <https://doi.org/10.1089/cmb.2012.0021>.
- Barchi, L., Acquadro, A., Alonso, D. *et al.* (2019a) Single Primer Enrichment Technology (SPET) for high-throughput genotyping in tomato and eggplant germplasm. *Front. Plant Sci.*, **10**. <https://doi.org/10.3389/fpls.2019.01005>.
- Barchi, L., Lanteri, S., Portis, E., Valè, G., Volante, A., Pulcini, L. *et al.* (2012) A RAD tag derived marker based eggplant linkage map and the location of QTLs determining anthocyanin pigmentation. *PLoS One*, **7**, e43740. <https://doi.org/10.1371/journal.pone.0043740>.
- Barchi, L., Pietrella, M., Venturini, L., Minio, A., Toppino, L., Acquadro, A. *et al.* (2019b) A chromosome-anchored eggplant genome sequence reveals key events in Solanaceae evolution. *Scientific Reports*, **9**, 11769. <https://doi.org/10.1038/s41598-019-47985-w>.
- Barchi, L., Toppino, L., Valentino, D., Bassolino, L., Portis, E., Lanteri, S. *et al.* (2018) QTL analysis reveals new eggplant loci involved in resistance to fungal wilts. *Euphytica*, **214**, 20. <https://doi.org/10.1007/s10681-017-2102-2>.
- Bellucci, E., Bitocchi, E., Ferrarini, A., Benazzo, A., Biagetti, E., Klie, S. *et al.* (2014) Decreased nucleotide and expression diversity and modified coexpression patterns characterize domestication in the common bean. *The Plant Cell*, **26**, 1901–1912. <https://doi.org/10.1105/tpc.114.124040>.
- Bromberg, Y. & Rost, B. (2007) SNAP: predict effect of non-synonymous polymorphisms on function. *Nucleic acids research*, **35**, 3823–3835.
- Brudno, M., Malde, S., Poliakov, A., Do, C.B., Couronne, O., Dubchak, I. *et al.* (2003) Glocal alignment: finding rearrangements during alignment. *Bioinformatics (Oxford, England)*, **19**(Suppl 1), i54–62. <https://doi.org/10.1093/bioinformatics/btg1005>.
- Burton, J.N., Adey, A., Patwardhan, R.P., Qiu, R., Kitzman, J.O. & Shendure, J. (2013) Chromosome-scale scaffolding of de novo genome assemblies based on chromatin interactions. *Nature Biotechnology*, **31**, 1119–1125. <https://doi.org/10.1038/nbt.2727>.
- Camacho, C., Coulouris, G., Avagyan, V., Ma, N., Papadopoulos, J., Bealer, K. *et al.* (2009) BLAST+: architecture and applications. *BMC Bioinformatics*, **10**, 421. <https://doi.org/10.1186/1471-2105-10-421>.
- Campbell, M.S., Law, MeiYee, Holt, C., Stein, J.C., Moghe, G.D., Hufnagel, D.E. *et al.* (2014) MAKER-P: a tool kit for the rapid creation, management, and quality control of plant genome annotations. *Plant physiology*, **164**, 513–524. <https://doi.org/10.1104/pp.113.230144>.
- Cericola, F., Portis, E., Lanteri, S., Toppino, L., Barchi, L., Acciarri, N. *et al.* (2014) Linkage disequilibrium and genome-wide association analysis for anthocyanin pigmentation and fruit color in eggplant. *BMC genomics*, **15**, 896. <https://doi.org/10.1186/1471-2164-15-896>.
- Chao, A. (1987) Estimating the population size for capture-recapture data with unequal catchability. *Biometrics*, **43**, 783–791. <https://doi.org/10.2307/2531532>.
- Chapman, M.A. (Ed.) (2019) *The Eggplant Genome*. Cham, Switzerland: Springer International Publishing.

- Chen, H., Patterson, N. & Reich, D. (2010) Population differentiation as a test for selective sweeps. *Genome Research*, **20**, 393–402. <https://doi.org/10.1101/gr.100545.109>.
- Chung, H.J., Jung, J.D., Park, H.W., Kim, J.H., Cha, H.W., Min, S.R. *et al.* (2006) The complete chloroplast genome sequences of *Solanum tuberosum* and comparative analysis with Solanaceae species identified the presence of a 241-bp deletion in cultivated potato chloroplast DNA sequence. *Plant Cell Reports*, **25**, 1369–1379. <https://doi.org/10.1007/s00299-006-0196-4>.
- Contreras-Moreira, B., Cantalapiedra, C.P., Garcia-Pereira, M.J., Gordon, S.P., Vogel, J.P., Igartua, E. *et al.* (2017) Analysis of plant pan-genomes and transcriptomes with GET_HOMOLOGUES-EST, a clustering solution for sequences of the same species. *Frontiers in Plant Science*, **8**, 184. <https://doi.org/10.3389/fpls.2017.00184>.
- Danecek, P., Auton, A., Abecasis, G., Albers, C.a., Banks, E., DePristo, M.a. *et al.* (2011) The variant call format and VCFtools. *Bioinformatics*, **27**, 2156–2158. <https://doi.org/10.1093/bioinformatics/btr330>.
- Daunay, M.C., Lester, R.N. & Anó, G. (2001a) Cultivated eggplants. In: Charrier, A., Jacquot, M., Hamon, S. & Nicolas, D. (Eds.) *Tropical Plant Breeding*. Oxford: Oxford University Press, pp. 200–225.
- Daunay, M.C., Lester, R.N., Gebhardt, C., Hennart, J.W. & Jahn, M. (2001b) Genetic resources of eggplant (*Solanum melongena*) and allied species: a new challenge for molecular geneticists and eggplant breeders. In R.G. van den Berg and G.W.M. Barendse, van der Weerden G.M., eds. *Solanaceae V: Advances in Taxonomy and Utilization*. pp. 251–274. Nijmegen: Nijmegen University Press.
- Ding, Q.-X., Liu, J. & Gao, L. (2016) The complete chloroplast genome of eggplant (*Solanum melongena* L.). *Mitochondrial DNA Part B*, **1**, 843–844. <https://doi.org/10.1080/23802359.2016.1186510>.
- Doganlar, S., Frary, A., Daunay, M.-C., Huvenaars, K., Mank, R. & Frary, A. (2014) High resolution map of eggplant (*Solanum melongena*) reveals extensive chromosome rearrangement in domesticated members of the Solanaceae. *Euphytica*, **198**, 231–241. <https://doi.org/10.1007/s10681-014-1096-2>.
- Doganlar, S., Frary, A., Daunay, M.-C.-C., Lester, R.N. & Tanksley, S.D. (2002a) A comparative genetic linkage map of eggplant (*Solanum melongena*) and its implications for genome evolution in the Solanaceae. *Genetics*, **161**, 1697–1711.
- Doganlar, S., Frary, A., Daunay, M.-C.-C., Lester, R.N. & Tanksley, S.D. (2002b) Conservation of gene function in the Solanaceae as revealed by comparative mapping of domestication traits in eggplant. *Genetics*, **161**, 1713–1726.
- FAO <http://faostat3.fao.org/home/E.org/>
- Francisco, R.M., Regalado, A., Ageorges, A. *et al.* (2013) ABC1, an ATP Binding cassette protein from grape berry, transports anthocyanidin 3-O-glucosides. *The Plant Cell*, **25**, 1840–1854. <https://doi.org/10.1105/tpc.112.102152>.
- Frary, A., Doganlar, S., Daunay, M.C. & Tanksley, S.D. (2003) QTL analysis of morphological traits in eggplant and implications for conservation of gene function during evolution of solanaceous species. *TAG Theoretical and Applied Genetics*, **107**, 359–370. <https://doi.org/10.1007/s00122-003-1257-5>.
- Frary, A., Frary, A., Daunay, M.-C., Huvenaars, K., Mank, R. & Doganlar, S. (2014) QTL hotspots in eggplant (*Solanum melongena*) detected with a high resolution map and CIM analysis. *Euphytica*, **197**, 211–228. <https://doi.org/10.1007/s10681-013-1060-6>.
- Frazer, K.A., Pachter, L., Poliakov, A., Rubin, E.M. & Dubchak, I. (2004) VISTA: computational tools for comparative genomics. *Nucleic acids research*, **32**, W273–W279. <https://doi.org/10.1093/nar/gkh458>.
- Fu, L., Niu, B., Zhu, Z., Wu, S. & Li, W. (2012) CD-HIT: accelerated for clustering the next-generation sequencing data. *Bioinformatics*, **28**, 3150–3152. <https://doi.org/10.1093/bioinformatics/bts565>.
- Fukuoka, H., Miyatake, K., Nunome, T., Negoro, S., Shirasawa, K., Isobe, S. *et al.* (2012) Development of gene-based markers and construction of an integrated linkage map in eggplant by using Solanum orthologous (SOL) gene sets. *Theoretical and Applied Genetics*, **125**, 47–56. <https://doi.org/10.1007/s00122-012-1815-9>.
- Gao, L., Gonda, I., Sun, H., Ma, Q., Bao, K., Tieman, D.M. *et al.* (2019) The tomato pan-genome uncovers new genes and a rare allele regulating fruit flavor. *Nature Genetics*, **51**, 1044–1051. <https://doi.org/10.1038/s41588-019-0410-2>.
- Golicz, A.A., Bayer, P.E., Barker, G.C., Edger, P.P., Kim, HyeRan, Martinez, P.A. *et al.* (2016) The pangenome of an agronomically important crop plant Brassica oleracea. *Nature Communications*, **7**, 1–8. <https://doi.org/10.1038/ncomms13390>.
- Golicz, A.A., Martinez, P.A., Zander, M., Patel, D.A., Van De Wouw, A.P., Visendi, P. *et al.* (2015) Gene loss in the fungal canola pathogen *Leptosphaeria maculans*. *Functional and Integrative Genomics*, **15**, 189–196. <https://doi.org/10.1007/s10142-014-0412-1>.
- Gordon, S.P., Contreras-Moreira, B., Woods, D.P., Des Marais, D.L., Burgess, D., Shu, S. *et al.* (2017) Extensive gene content variation in the *Brachypodium distachyon* pan-genome correlates with population structure. *Nature Communications*, **8**, 2184. <https://doi.org/10.1038/s41467-017-02292-8>.
- Gramazio, P., Prohens, J., Plazas, M., Andújar, I., Herraiz, F.J., Castillo, E. *et al.* (2014) Location of chlorogenic acid biosynthesis pathway and polyphenol oxidase genes in a new interspecific anchored linkage map of eggplant. *BMC Plant Biology*, **14**, 350. <https://doi.org/10.1186/s12870-014-0350-z>.
- Gramazio, P., Yan, H., Hasing, T., Vilanova, S., Prohens, J. & Bombarely, A. (2019) Whole-genome resequencing of seven eggplant (*Solanum melongena*) and one wild relative (*S. incanum*) accessions provides new insights and breeding tools for eggplant enhancement. *Frontiers in Plant Science*, **10**. <https://doi.org/10.3389/fpls.2019.01222>.
- Greiner, S., Lehwark, P. & Bock, R. (2019) OrganellarGenomeDRAW (OGDRAW) version 1.3.1: expanded toolkit for the graphical visualization of organellar genomes. *Nucleic Acids Research*, **47**, W59–W64. <https://doi.org/10.1093/nar/gkz238>.
- Hancock, K.R., Collette, V., Fraser, K., Greig, M., Xue, H., Richardson, K. *et al.* (2012) Expression of the R2R3-MYB transcription factor TaMYB14 from *Trifolium arvense* activates proanthocyanidin biosynthesis in the legumes *Trifolium repens* and *Medicago sativa*. *Plant Physiology*, **159**, 1204–1220. <https://doi.org/10.1104/pp.112.195420>.
- Himmelbach, A., Ruban, A., Walde, I., Šimková, H., Doležel, J., Hastie, A. *et al.* (2018) Discovery of multi-megabase polymorphic inversions by chromosome conformation capture sequencing in large-genome plant species. *The Plant Journal*, **96**, 1309–1316. <https://doi.org/10.1111/tbj.14109>.
- Hirakawa, H., Shirasawa, K., Miyatake, K., Nunome, T., Negoro, S., Ohyama, A. *et al.* (2014) Draft genome sequence of eggplant (*Solanum melongena* L.): the representative solanum species indigenous to the old world. *DNA Research : An International Journal for Rapid Publication of Reports on Genes and Genomes*, **21**, 649–660. <https://doi.org/10.1093/dnares/dsu027>.
- Hoang, D.T., Chernomor, O., von Haeseler, A., Minh, B.Q. & Vinh, L.S. (2018) UFBoot2: improving the ultrafast bootstrap approximation. *Molecular Biology and Evolution*, **35**, 518–522. <https://doi.org/10.1093/molbev/msx281>.
- Hollingsworth, P.m., Forrest, L.I., Spouge, J.I., Hajibabaei, M., Ratnasingham, S., van der Bank, M. *et al.* (2009) A DNA barcode for land plants. *Proceedings of the National Academy of Sciences of the United States of America*, **106**, 12794–12797. <https://doi.org/10.1073/pnas.0905845106>.
- Hu, M., Deng, K., Selvaraj, S., Qin, Z., Ren, B. & Liu, J.S. (2012) HiCNorm: removing biases in Hi-C data via Poisson regression. *Bioinformatics*, **28**, 3131–3133. <https://doi.org/10.1093/bioinformatics/bts570>.
- Hurgobin, B., Golicz, A.A., Bayer, P.E. *et al.* (2018) Homoeologous exchange is a major cause of gene presence/absence variation in the amphidiploid *Brassica napus*. *Plant Biotechnology Journal*, **16**, 1265–1274. <https://doi.org/10.1111/pbi.12867>.
- Jaakola, L., Määttä, K., Pirttilä, A.M., Törrönen, R., Kärenlampi, S. & Hohola, A. (2002) Expression of genes involved in anthocyanin biosynthesis in relation to anthocyanin, proanthocyanidin, and flavonol levels during bilberry fruit development. *Plant Physiology*, **130**, 729–739. <https://doi.org/10.1104/pp.006957>.
- Jin, J.-J., Yu, W.-B., Yang, J.-B., Song, Y., Yi, T.-S. & Li, D.-Z. (2018) GetOrganelle: a simple and fast pipeline for de novo assembly of a complete circular chloroplast genome using genome skimming data. *bioRxiv*, 256479. <https://doi.org/10.1101/256479>.
- Jones, P., Binns, D., Chang, H.-y., Fraser, M., Li, W., McAnulla, C. *et al.* (2014) InterProScan 5: genome-scale protein function classification. *Bioinformatics (Oxford, England)*, **30**, 1236–1240. <https://doi.org/10.1093/bioinformatics/btu031>.

- Kahlau, S., Aspinall, S., Gray, J.C. & Bock, R. (2006) Sequence of the tomato chloroplast DNA and evolutionary comparison of solanaceous plastid genomes. *Journal of Molecular Evolution*, **63**, 194–207. <https://doi.org/10.1007/s00239-005-0254-5>.
- Katoh, K. & Standley, D.M. (2013) MAFFT multiple sequence alignment software version 7: improvements in performance and usability. *Molecular biology and evolution*, **30**, 772–780. <https://doi.org/10.1093/molbev/mst010>.
- Kaushik, P., Gramazio, P., Vilanova, S., Raigón, M.D., Prohens, J. & Plazas, M. (2017) Phenolics content, fruit flesh colour and browning in cultivated eggplant, wild relatives and interspecific hybrids and implications for fruit quality breeding. *Food Research International*, **102**, 392–401. <https://doi.org/10.1016/j.foodres.2017.09.028>.
- Kim, S., Park, J., Yeom, S.-I., Kim, Y.-M., Seo, E., Kim, K.-T. et al. (2017) New reference genome sequences of hot pepper reveal the massive evolution of plant disease-resistance genes by retroduplication. *Genome Biology*, **18**, 210. <https://doi.org/10.1186/s13059-017-1341-9>.
- Knapp, S., Aubriot, X. & Prohens, J. (2019) Eggplant (*Solanum melongena* L.): taxonomy and relationships. In: Chapman, M.A. (Ed.) *The Eggplant Genome*. Compendium of Plant Genomes. Cham: Springer International Publishing, pp. 11–22. https://doi.org/10.1007/978-3-319-99208-2_2.
- Knapp, S., Vorontsova, M.S. & Prohens, J. (2013) Wild Relatives of the eggplant (*Solanum melongena* L.: Solanaceae): new understanding of species names in a complex group. *PLoS One*, **8**, e57039. <https://doi.org/10.1371/journal.pone.0057039>.
- Kofler, R., Schlötterer, C. & Lelley, T. (2007) SciRoKo: a new tool for whole genome microsatellite search and investigation. *Bioinformatics*, **23**, 1683–1685. <https://doi.org/10.1093/bioinformatics/btm157>.
- Kozlov, A.M., Darriba, D., Flouri, T., Morel, B. & Stamatakis, A. (2019) RAXML-NG: a fast, scalable and user-friendly tool for maximum likelihood phylogenetic inference. *Bioinformatics*, **35**, 4453–4455. <https://doi.org/10.1093/bioinformatics/btz305>.
- Kurtz, S., Choudhuri, J.V., Ohlebusch, E., Schleiermacher, C., Stoye, J. & Giegerich, R. (2001) REPuter: the manifold applications of repeat analysis on a genomic scale. *Nucleic Acids Research*, **29**, 4633–4642. <https://doi.org/10.1093/nar/29.22.4633>.
- Lakušić, D., Liber, Z., Nikolić, T., Surina, B., Kovacčić, S., Bogdanović, S. et al. (2013) Molecular phylogeny of the *Campanula pyramidalis* species complex (Campanulaceae) inferred from chloroplast and nuclear non-coding sequences and its taxonomic implications. *Taxon*, **62**, 505–524. <https://doi.org/10.12705/623.1>.
- Lamesch, P., Berardini, T.Z., Li, D., Swarbreck, D., Wilks, C., Sasidharan, R. et al. (2012) The Arabidopsis Information Resource (TAIR): improved gene annotation and new tools. *Nucleic Acids Research*, **40**, D1202–D1210. <https://doi.org/10.1093/nar/gkr1090>.
- Li, D., Liu, C.-M., Luo, R., Sadakane, K. & Lam, T.-W. (2015) MEGAHIT: an ultra-fast single-node solution for large and complex metagenomics assembly via succinct de Bruijn graph. *Bioinformatics*, **31**, 1674–1676. <https://doi.org/10.1093/bioinformatics/btv033>.
- Li, H. (2011) A statistical framework for SNP calling, mutation discovery, association mapping and population genetical parameter estimation from sequencing data. *Bioinformatics (Oxford, England)*, **27**, 2987–2993. <https://doi.org/10.1093/bioinformatics/btr509>.
- Li, H. (2013) Aligning sequence reads, clone sequences and assembly contigs with BWA-MEM. *Genomics*, 1303.
- Li, H. (2018) Minimap2: pairwise alignment for nucleotide sequences. *Bioinformatics*, **34**, 3094–3100. <https://doi.org/10.1093/bioinformatics/bty191>.
- Liu, W., Chen, L., Zhang, S., Hu, F., Wang, Z., Lyu, J. et al. (2019) Decrease of gene expression diversity during domestication of animals and plants. *BMC Evolutionary Biology*, **19**, 19. <https://doi.org/10.1186/s12862-018-1340-9>.
- Magdy, M., Ou, L., Yu, H., Chen, R., Zhou, Y., Hassan, H. et al. (2019) Pan-plastome approach empowers the assessment of genetic variation in cultivated Capsicum species. *Horticulture Research*, **6**, 108. <https://doi.org/10.1038/s41438-019-0191-x>.
- Mangino, G., Plazas, M., Vilanova, S., Prohens, J. & Gramazio, P. (2020) Performance of a set of eggplant (*Solanum melongena*) lines with introgressions from its wild relative *S. incanum* under open field and greenhouse conditions and detection of QTLs. *Agronomy*, **10**, 467. <https://doi.org/10.3390/agronomy10040467>.
- Mangino, G., Vilanova, S., Plazas, M., Prohens, J. & Gramazio, P. (2021) Fruit shape morphometric analysis and QTL detection in a set of eggplant introgression lines. *Scientia Horticulturae*, **282**, 110006. <https://doi.org/10.1016/j.scienta.2021.110006>.
- Mascher, M., Gundlach, H., Himmelbach, A., Beier, S., Twardziok, S.O., Wicker, T. et al. (2017) A chromosome conformation capture ordered sequence of the barley genome. *Nature*, **544**, 427–433. <https://doi.org/10.1038/nature22043>.
- Millen, R.S., Olmstead, R.G., Adams, K.L. et al. (2001) Many parallel losses of infa from chloroplast dna during angiosperm evolution with multiple independent transfers to the nucleus. *The Plant Cell*, **13**, 645–658. <https://doi.org/10.1105/tpc.13.3.645>.
- Minh, B.Q., Schmidt, H.A., Chernomor, O., Schrempf, D., Woodhams, M.D., von Haeseler, A. et al. (2020) IQ-TREE 2: new models and efficient methods for phylogenetic inference in the genomic era. *Molecular Biology and Evolution*, **37**, 1530–1534. <https://doi.org/10.1093/molbev/msaa015>.
- Miyatake, K., Saito, T., Negoro, S., Yamaguchi, H., Nunome, T., Ohyama, A. et al. (2012) Development of selective markers linked to a major QTL for parthenocarp in eggplant (*Solanum melongena* L.). *TAG Theoretical and Applied Genetics*, **124**, 1–11. <https://doi.org/10.1007/s00122-012-1796-8>.
- Miyatake, K., Saito, T., Nunome, T., Yamaguchi, H., Negoro, S., Ohyama, A. et al. (2020) Fine mapping of a major locus representing the lack of prickles in eggplant revealed the availability of a 0.5-kb insertion/deletion for marker-assisted selection. *Breeding Science*, **70**, 438–448. <https://doi.org/10.1270/jsbbs.20004>.
- Moglia, A., Florio, F.E., Iacopino, S. et al. (2020) Identification of a new R3 MYB type repressor and functional characterization of the members of the MBW transcriptional complex involved in anthocyanin biosynthesis in eggplant (*S. melongena* L.) S. Aceto, ed. *PLoS One*, **15**, e0232986. <https://doi.org/10.1371/journal.pone.0232986>.
- Monat, C., Padmarasu, S., Lux, T., Wicker, T., Gundlach, H., Himmelbach, A. et al. (2019) TRITEX: chromosome-scale sequence assembly of Triticeae genomes with open-source tools. *Genome Biology*, **20**, 284. <https://doi.org/10.1186/s13059-019-1899-5>.
- Movahed, N., Pastore, C., Cellini, A., Allegro, G., Valentini, G., Zenoni, S. et al. (2016) The grapevine *VviPrx31* peroxidase as a candidate gene involved in anthocyanin degradation in ripening berries under high temperature. *Journal of Plant Research*, **129**, 513–526. <https://doi.org/10.1007/s10265-016-0786-3>.
- Mu, Q., Huang, Z., Chakrabarti, M., Illa-Berenguer, E., Liu, X., Wang, Y. et al. (2017) Fruit weight is controlled by *Cell Size Regulator* encoding a novel protein that is expressed in maturing tomato fruits. *PLOS Genetics*, **13**, e1006930. <https://doi.org/10.1371/journal.pgen.1006930>.
- Muñoz, S., Ranc, N., Botton, E., Bérard, A., Rolland, S., Duffé, P. et al. (2011) Increase in tomato locule number is controlled by two single-nucleotide polymorphisms located near *WUSCHEL*. *Plant Physiology*, **156**, 2244–2254.
- Nguyen, L.-T., Schmidt, H.A., von Haeseler, A. & Minh, B.Q. (2015) IQ-TREE: a fast and effective stochastic algorithm for estimating maximum-likelihood phylogenies. *Molecular Biology and Evolution*, **32**, 268–274. <https://doi.org/10.1093/molbev/msu300>.
- Nunome, T., Ishiguro, K., Yoshida, T. & Hirai, M. (2001) Mapping of fruit shape and color development traits in eggplant (*Solanum melongena* L.) based on RAPD and AFLP markers. *Breeding science*, **51**, 19–26.
- Nunome, T., Negoro, S., Kono, I., Kanamori, H., Miyatake, K., Yamaguchi, H. et al. (2009) Development of SSR markers derived from SSR-enriched genomic library of eggplant (*Solanum melongena* L.). *Theoretical and applied genetics*, **119**, 1143–1153. <https://doi.org/10.1007/s00122-009-1116-0>.
- Ou, L., Li, D., Lv, J., Chen, W., Zhang, Z., Li, X. et al. (2018) Pan-genome of cultivated pepper (*Capsicum*) and its use in gene presence-absence variation analyses. *New Phytologist*, **220**, 360–363. <https://doi.org/10.1111/nph.15413>.
- Padmarasu, S., Himmelbach, A., Mascher, M. & Stein, N. (2019) In Situ Hi-C for plants: an improved method to detect long-range chromatin interactions. In: Chekanova, J.A. & Wang, H.-L.-V. (Eds.) *Plant Long Non-Coding RNAs: Methods and Protocols*. Methods in Molecular Biology. New York: Springer, pp. 441–472. https://doi.org/10.1007/978-1-4939-9045-0_28.
- Page, A., Gibson, J., Meyer, R.S. & Chapman, M.A. (2019) Eggplant domestication: pervasive gene flow, feralization, and transcriptomic divergence.

- Molecular Biology and Evolution*, **36**, 1359–1372. <https://doi.org/10.1093/molbev/msz062>.
- Parks, M., Cronn, R. & Liston, A.** (2009) Increasing phylogenetic resolution at low taxonomic levels using massively parallel sequencing of chloroplast genomes. *BMC Biology*, **7**, 84. <https://doi.org/10.1186/1741-7007-7-84>.
- Pattengale, N.D., Alipour, M., Bininda-Emonds, O.R.P., Moret, B.M.E. & Stamatakis, A.** (2010) How many bootstrap replicates are necessary? In *Journal of Computational Biology*. Mary Ann Liebert, Inc. Rochelle, NY, pp. 337–354. <https://doi.org/10.1089/cmb.2009.0179>.
- Pérez-Díaz, R., Rynhajillo, M., Pérez-Díaz, J., Peña-Cortés, H., Casaretto, J.A., González-Villanueva, E. et al.** (2014) VvMATE1 and VvMATE2 encode putative proanthocyanidin transporters expressed during berry development in *Vitis vinifera* L. *Plant Cell Reports*, **33**, 1147–1159. <https://doi.org/10.1007/s00299-014-1604-9>.
- Portis, E., Barchi, L., Toppino, L., Lanteri, S., Acciarri, N., Felicioni, N. et al.** (2014) QTL mapping in eggplant reveals clusters of yield-related loci and orthology with the tomato genome. *PLoS One*, **9**, e89499. <https://doi.org/10.1371/journal.pone.0089499>.
- Portis, E., Cericola, F., Barchi, L., Toppino, L., Acciarri, N., Pulcini, L. et al.** (2015) Association mapping for fruit, plant and leaf morphology traits in eggplant. *PLoS One*, **10**, e0135200. <https://doi.org/10.1371/journal.pone.0135200>.
- Pracana, R., Priyam, A., Levantis, I., Nichols, R.A. & Wurm, Y.** (2017) The fire ant social chromosome supergene variant *Sb* shows low diversity but high divergence from *SB*. *Molecular Ecology*, **26**, 2864–2879. <https://doi.org/10.1111/mec.14054>.
- Quinlan, A.R. & Hall, I.M.** (2010) BEDTools: a flexible suite of utilities for comparing genomic features. *Bioinformatics (Oxford, England)*, **26**, 841–842. <https://doi.org/10.1093/bioinformatics/btq033>.
- R Core Team** (2020) *R: A Language and Environment for Statistical Computing*. Vienna, Austria: R Foundation for Statistical Computing.
- Ranil, R.h.g., Prohens, J., Aubriot, X., Niran, H.m.l., Plazas, M., Fonseca, R.m. et al.** (2017) *Solanum insanum* L. (subgenus *Leptostemonum* Bitter, Solanaceae), the neglected wild progenitor of eggplant (*S. melongena* L.): a review of taxonomy, characteristics and uses aimed at its enhancement for improved eggplant breeding. *Genetic Resources and Crop Evolution*, **64**, 1707–1722. <https://doi.org/10.1007/s10722-016-0467-z>.
- Rasko, D.A., Rosovitz, M.J., Myers, G.S.A., Mongodin, E.F., Fricke, W.F., Gajer, P. et al.** (2008) The pangenome structure of *Escherichia coli*: comparative genomic analysis of *E. coli* commensal and pathogenic isolates. *Journal of Bacteriology*, **190**, 6881–6893. <https://doi.org/10.1128/JB.00619-08>.
- Revell, L.J.** (2012) phytools: an R package for phylogenetic comparative biology (and other things): *phytools: R package. Methods in Ecology and Evolution*, **3**, 217–223. <https://doi.org/10.1111/j.2041-210X.2011.00169.x>.
- Rodríguez, G.R., Muñoz, S., Anderson, C., Sim, S.-C., Michel, A., Causse, M. et al.** (2011) Distribution of *SUN*, *OVATE*, *LC*, and *FAS* in the tomato germplasm and the relationship to fruit shape diversity. *Plant Physiology*, **156**, 275–285. <https://doi.org/10.1104/pp.110.167577>.
- Rozas, J., Ferrer-Mata, A., Sánchez-DelBarrio, J.C., Guirao-Rico, S., Librado, P., Ramos-Onsins, S.E. et al.** (2017) DnaSP 6: DNA sequence polymorphism analysis of large data sets. *Molecular Biology and Evolution*, **34**, 3299–3302. <https://doi.org/10.1093/molbev/msx248>.
- Salgon, S., Raynal, M., Lebon, S., Baptiste, J.M., Daunay, M.C., Dintinger, J. et al.** (2018) Genotyping by sequencing highlights a polygenic resistance to *Ralstonia pseudosolanacearum* in eggplant (*Solanum melongena* L.). *International Journal of Molecular Sciences*, **19**, 357. <https://doi.org/10.3390/ijms19020357>.
- Shaw, J., Lickey, E.B., Beck, J.T., Farmer, S.B., Liu, W., Miller, J. et al.** (2005) The tortoise and the hare II: relative utility of 21 noncoding chloroplast DNA sequences for phylogenetic analysis. *American Journal of Botany*, **92**, 142–166. <https://doi.org/10.3732/ajb.92.1.142>.
- Simão, F.A., Waterhouse, R.M., Ioannidis, P., Kriventseva, E.V. & Zdobnov, E.M.** (2015) BUSCO: assessing genome assembly and annotation completeness with single-copy orthologs. *Bioinformatics*, **31**, 3210–3212. <https://doi.org/10.1093/bioinformatics/btv351>.
- Snipen, L. & Liland, K.H.** (2015) Micropan: an R-package for microbial pan-genomics. *BMC Bioinformatics*, **16**, 79. <https://doi.org/10.1186/s12859-015-0517-0>.
- Song, B.o., Song, Y., Fu, Y., Kizito, E.B., Kamenya, S.N., Kabod, P.N. et al.** (2019) Draft genome sequence of *Solanum aethiopicum* provides insights into disease resistance, drought tolerance, and the evolution of the genome. *GigaScience*, **8**, giz115. <https://doi.org/10.1093/gigascience/giz115>.
- Stanke, M., Keller, O., Gunduz, I., Hayes, A., Waack, S. & Morgenstern, B.** (2006) AUGUSTUS: ab initio prediction of alternative transcripts. *Nucleic Acids Research*, **34**, W435–W439. <https://doi.org/10.1093/nar/gkl200>.
- Tettelin, H., Massignani, V., Cieslewicz, M.J., Donati, C., Medini, D., Ward, N.I. et al.** (2005) Genome analysis of multiple pathogenic isolates of *Streptococcus agalactiae*: implications for the microbial "pan-genome". *Proceedings of the National Academy of Sciences*, **102**(39), 13950–13955.
- Tettelin, H., Riley, D., Cattuto, C. & Medini, D.** (2008) Comparative genomics: the bacterial pan-genome. *Current Opinion in Microbiology*, **11**, 472–477. <https://doi.org/10.1016/j.mib.2008.09.006>.
- The Tomato Genome Consortium** (2012) The tomato genome sequence provides insights into fleshy fruit evolution. *Nature*, **485**, 635–641. <https://doi.org/10.1038/nature11119>.
- The UniProt Consortium** (2014) UniProt: a hub for protein information. *Nucleic Acids Research*, **43**, D204–212. <https://doi.org/10.1093/nar/gku989>.
- Tian, T., Liu, Y., Yan, H., You, Q., Yi, X., Du, Z. et al.** (2017) agriGO v2.0: a GO analysis toolkit for the agricultural community, 2017 update. *Nucleic Acids Research*, **45**, W122–W129. <https://doi.org/10.1093/nar/gkx382>.
- Tillich, M., Lehwark, P., Pellizzer, T., Ulbricht-Jones, E.S., Fischer, A., Bock, R. et al.** (2017) GeSeq – versatile and accurate annotation of organelle genomes. *Nucleic Acids Research*, **45**, W6–W11. <https://doi.org/10.1093/nar/gkx391>.
- Toppino, L., Barchi, L., Lo Scalzo, R. et al.** (2016) Mapping Quantitative Trait Loci affecting biochemical and morphological fruit properties in eggplant (*Solanum melongena* L.). *Frontiers in Plant Science*. <https://doi.org/10.3389/fpls.2016.00256>.
- Toppino, L., Barchi, L., Mercati, F., Acciarri, N., Perrone, D., Martina, M. et al.** (2020) A new intra-specific and high-resolution genetic map of eggplant based on a RIL Population, and location of QTLs related to plant anthocyanin pigmentation and seed vigour. *Genes*, **11**, 745. <https://doi.org/10.3390/genes11070745>.
- Toppino, L., Vale, G. & Rotino, G.L.** (2008) Inheritance of *Fusarium* wilt resistance introgressed from *Solanum aethiopicum* Gilo and *Aculeatum* groups into cultivated eggplant (*S. melongena*) and development of associated PCR-based markers. *Molecular Breeding*, **22**, 237–250.
- van der Knaap, E. & Østergaard, L.** (2018) Shaping a fruit: developmental pathways that impact growth patterns. *Seminars in Cell & Developmental Biology*, **79**, 27–36. <https://doi.org/10.1016/j.semdev.2017.10.028>.
- Vorontsova, M.S. & Knapp, S.** (2016) A revision of the "spiny *Solanums*," *Solanum* subgenus *Leptostemonum* (Solanaceae), in Africa and Madagascar. *Systematic Botany Monographs*, Vol. **99**, pp. 1–432.
- Vorontsova, M.S., Stern, S., Bohs, L. & Knapp, S.** (2013) African spiny *Solanum* (subgenus *Leptostemonum*, Solanaceae): a thorny phylogenetic tangle. *Botanical Journal of the Linnean Society*, **173**, 176–193. <https://doi.org/10.1111/boj.12053>.
- Wang, Z., Yang, Z. & Li, F.** (2019) Updates on molecular mechanisms in the development of branched trichome in Arabidopsis and nonbranched in cotton. *Plant Biotechnology Journal*, **17**, 1706–1722. <https://doi.org/10.1111/pbi.13167>.
- Wei, Q., Wang, J., Wang, W., Hu, T., Hu, H. & Bao, C.** (2020a) A high-quality chromosome-level genome assembly reveals genetics for important traits in eggplant. *Horticulture Research*, **7**, 1–15. <https://doi.org/10.1038/s41438-020-00391-0>.
- Wei, Q., Wang, W., Hu, T., Hu, H., Wang, J. & Bao, C.** (2020b) Construction of a SNP-based genetic map using SLAF-Seq and QTL analysis of morphological traits in eggplant. *Frontiers in Genetics*, **11**, 178. <https://doi.org/10.3389/fgene.2020.00178>.
- Weir, B.S. & Cockerham, C.C.** (1984) Estimating F-statistics for the analysis of population structure. *Evolution*, **38**, 1358–1370.
- Wood, D.E., Lu, J. & Langmead, B.** (2019) Improved metagenomic analysis with Kraken 2. *Genome Biology*, **20**, 257. <https://doi.org/10.1101/762302>.
- Wu, Z.** (2016) The completed eight chloroplast genomes of tomato from *Solanum* genus. *Mitochondrial DNA Part A*, **27**, 4155–4157. <https://doi.org/10.3109/19401736.2014.1003890>.

- Xiao, X.O., Lin, Wq., Li, K., Feng, X.F., Jin, H. & Zou, Hf. (2018). Transcriptome analyses reveal anthocyanin biosynthesis in eggplants. *PeerJ Preprints*, 6:e27289v1
- Zhang, C., Dong, S.-S., Xu, J.-Y., He, W.-M. & Yang, T.-L. (2018a) PopLDdecay: a fast and effective tool for linkage disequilibrium decay analysis based on variant call format files. *Bioinformatics*, 35, 1786–1788. <https://doi.org/10.1093/bioinformatics/bty875>.
- Zhang, L., Sun, H., Xu, T., Shi, T., Li, Z. & Hou, W. (2021) Comparative transcriptome analysis reveals key genes and pathways involved in prickly development in eggplant. *Genes*, 12, 341. <https://doi.org/10.3390/genes12030341>.
- Zhang, R., Zhang, L., Wang, W., Zhang, Z., Du, H., Qu, Z. *et al.* (2018b) Differences in codon usage bias between photosynthesis-related genes and genetic system-related genes of chloroplast genomes in cultivated and wild solanum species. *International Journal of Molecular Sciences*, 19, 3142. <https://doi.org/10.3390/ijms19103142>.
- Zhang, Y., Hu, Z., Chu, G., Huang, C., Tian, S., Zhao, Z. *et al.* (2014) Anthocyanin accumulation and molecular analysis of anthocyanin biosynthesis-associated genes in eggplant (*Solanum melongena* L.). *Journal of Agricultural and Food Chemistry*, 62, 2906–2912. <https://doi.org/10.1021/jf404574c>.
- Zhao, Y., Jia, X., Yang, J., Ling, Y., Zhang, Z., Yu, J. *et al.* (2014) PanGP: a tool for quickly analyzing bacterial pan-genome profile. *Bioinformatics (Oxford, England)*, 30, 1297–1299. <https://doi.org/10.1093/bioinformatics/btu017>.
- Zheng, X., Levine, D., Shen, J., Gogarten, S.M., Laurie, C. & Weir, B.S. (2012) A high-performance computing toolset for relatedness and principal component analysis of SNP data. *Bioinformatics*, 28, 3326–3328. <https://doi.org/10.1093/bioinformatics/bts606>.